SINKING COOLING WATER PLUMES IN A NUMERICAL MODEL

By Jonny Svensson

SMHI Reports
HYDROLOGY AND OCEANOGRAPHY
No RHO 23 (1980)

SMHI
Sveriges meteorologiska och hydrologiska institut

Dnr 609/131

SINKING COOLING WATER PLUMES IN A NUMERICAL MODEL

By Jonny Svensson

SMHI Reports
HYDROLOGY AND OCEANOGRAPHY
No RHO 23 (1980)

SJUNKANDE KYLVATTENPLYMER I EN NUMERISK MODELL

SVERIGES METEOROLOGISKA OCH HYDROLOGISKA INSTITUT
Norrköping 1980

ISSN 0347-7827

SMHI

TABLE OF CONTENTS

ABSTRACT

Cooling water discharged from a power plant during winter conditions can form a mixture which is denser than the ambient cold water. The cooling water then sinks to the bottom. Such sinking plumes have been recorded during plume surveys outside power plants discharging in brackich or fresh waters.

A three-dimensional matematical numerical model is used to describe the sinking plume. The model runs show that the turbulence in the ambient water affects the sinking considerably. In rough weather conditions with strong turbulence the cooling water is well mixed from the surface to the bottom. A vertical wall (thermal bar) separates ambient water from cooling water. The warm water does not go very far from the outlet. During periods with low wind velocities (little turbulence in the ambient water) the model simulates both the initial floating plume, the sinking and the final spreading along the bottom.

Three runs are presented. One with straight coast and flat bottom. In this model configuration tests with different mixing coefficients were performed. The next run presented shows the small changes that occur when a simple bottom topography is introduced in the model. The final case is one with a complicated coastline and bottom topography.

The model is shown to be a valuable tool in the process of judging the frequenecy and duration of sinking plumes and the size of bottom area outside a powerplant that will be affected by cooling water.

PHYSICAL BACKGROUND OF SINKING PLUMES

Pure water has its maximum density at a temperature of 4°C. This density equals one g/cm^3 by definition of the unit gram. One cubic centimetre of water of higher and also lower temperature than 4°C is lighter than one gram. With increasing salinity the temperature of the density maximum of sea water decreases. At salinities of over 17 °/oo it drops below 0°C.

The temperature of the freezing point decreases with increasing salinity at a slower rate than the temperature of the density maximum, and at a salinity of 24.7 °/oo both temperatures are equal at - 1.33°C (figure 1). This property of water is very important for the heat exchange in the oceans. It also determines the behaviour of cooling water plumes in fresh or brackish waters. Water, initially of 10°C, that is discharged into ambient waters at freezing temperature, will sink down towards the bottom, when it is cooled to a level around the temperature for maximal density. The range, in which sinking can be expected, decreases with salinity. No pronounced sinking can be observed for salinities above about 15 °/oo, even if the temperature and salinity distribution indicate instability according to the condition for static stability:

$$\frac{1}{\rho}\frac{d\rho}{dz} = \frac{1}{\rho}\frac{\partial\rho}{\partial s}\frac{ds}{dz} + \frac{1}{\rho}\frac{\partial\rho}{\partial T}\frac{dT}{dz} > 0 \qquad \text{(z pos upwards)}$$

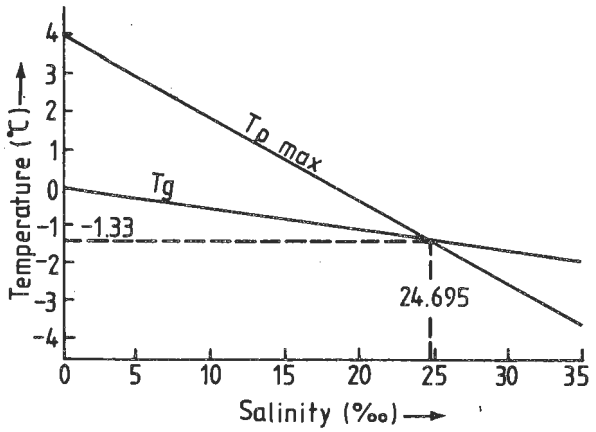

Fig 1 Temperature of the density maximum $T_{\rho\ max}$ and temperature of the freezing point, Tg for sea water of different temperature.

In fact instability associated with vertical overturning of water masses is more complicated, as heat conduction, friction and diffusion retard the motion and tend to stabilize it (Turner 1973). Neumann has indicated (Neumann - Pierson, 1966) that neutral stratification in the oceans can occur only when the vertical density gradient reaches a certain negative value or when:

$$\frac{1}{\rho}\frac{\partial \rho}{\partial s}\frac{ds}{dz} + \frac{1}{\rho}\frac{\partial \rho}{\partial T}\frac{dT}{dz} \geq \text{const} \cdot \frac{A \cdot K}{\rho^2 g h^4},$$

where A and K are turbulent viscosity and turbulent heat conductivity respectively, and h is the thickness of the layer, where the negative density gradient occur. The constant is of the order 10^3 in the oceans.

Suppose for a moment that one knows A and K. A = K = 0.001 m^2/s, the ambient water has the temperature 0^oC and the salinity 8 $^o/oo$, which gives the density ρ = 1.006400 g/cm^3. Part of a cooling water plume has the temperature 2.5^oC (ρ = = 1.006441 g/cm^3. The density difference is $4.1 \cdot 10^{-5}$ g/cm^3.

The formula $\frac{1}{\rho}\frac{\Delta \rho}{\Delta z} > \frac{10^3 \cdot AK}{\rho^2 g h^4}$ gives (if $\Delta z \approx h$) that the thickness of the unstable layer has to be of the order of magnitude of meters, before convection starts.

The Baltic Sea has a salinity and a winter temperature stratification that allows sinking cooling water plumes. Examples of this is given in the next section. The driving forces are weak, and the process can be disturbed by small natural density differences between the intake an the outlet area. "False" sinking plumes can for example be created on the west coast of Sweden.

OBSERVATIONS OF SINKING PLUMES

When the ambient temperature is low, the wind is weak, the sea state calm and the current weak, well defined sinking plumes have been observed. One example from outside Simpevarp is shown in figures 2 and 3. A few hundred meters outside Hamnehålet a remarkably well defined core of 6°C cooling water was observed. The sinking area was not larger than 100 m in diameter and the maximum temperature at the bottom 6°C. This means that the water in the center of the core was somewhat lighter than the ambient water of 0°C. The areas with an overtemperature of 1°C or more at the bottom were vast and could not be totally surveyed. No attempt was made to measure the vertical current. The cooling water flow from the nuclear power station was 22 m^3/s. The waste heat discharged was only 11 GWh/day.

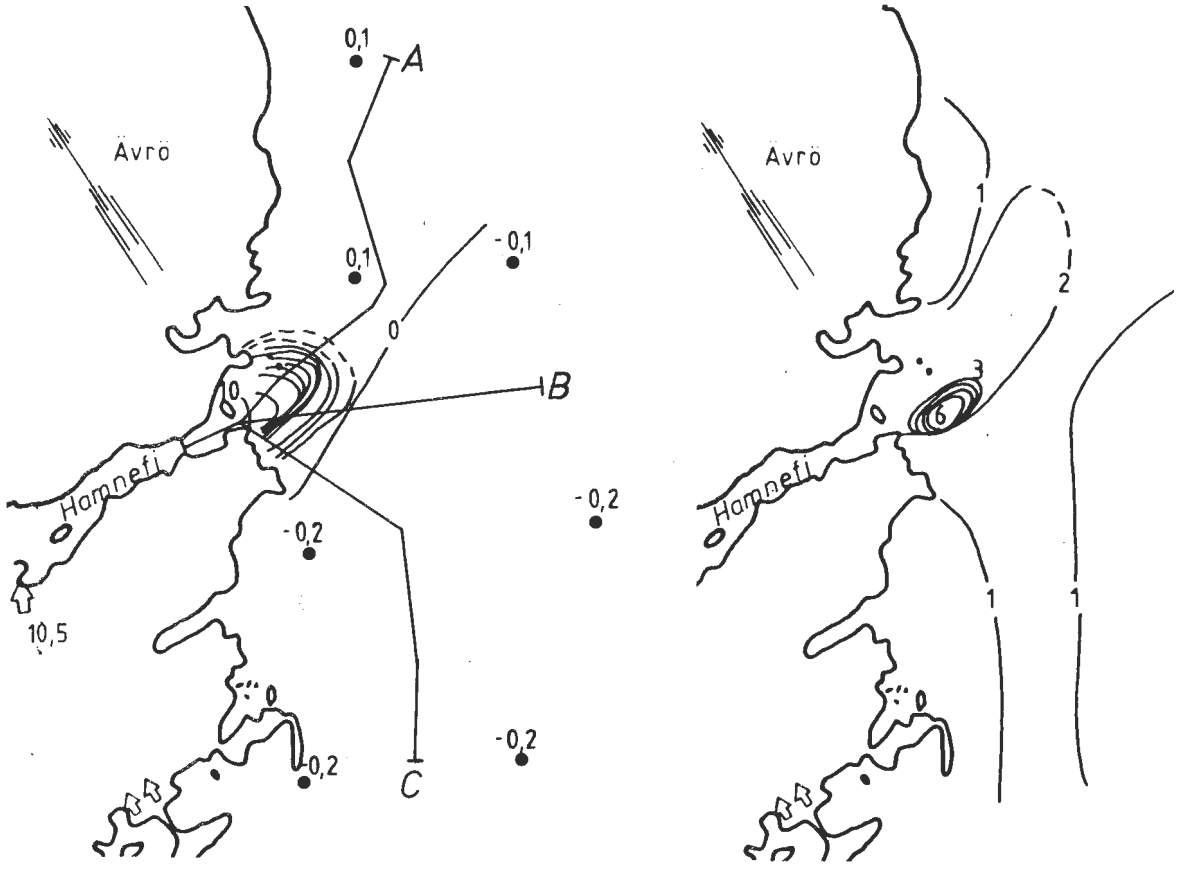

Fig. 2 Surface and bottom temperatures outside Oskarshamn Power Plant

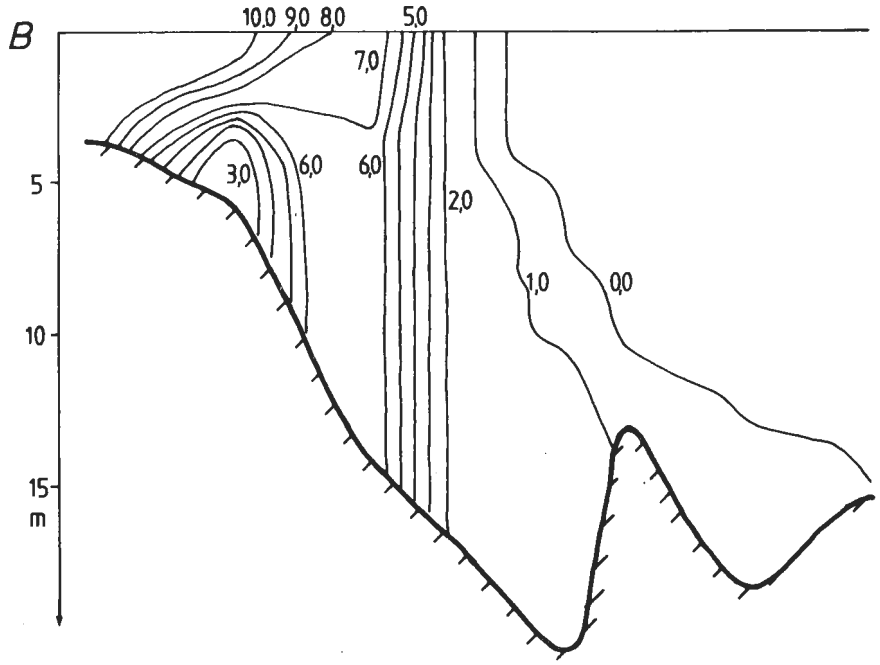

Fig. 3 Example of a sinking plume during calm weather conditions

Another example of a sinking plume from outside Karlshamnsverket is shown i figure 4. The ambient temperature was around 1.5°C and the temperature in the sinking core 4°C. The depth in the sinking area is only 5 - 10 m. No velocities were measured.

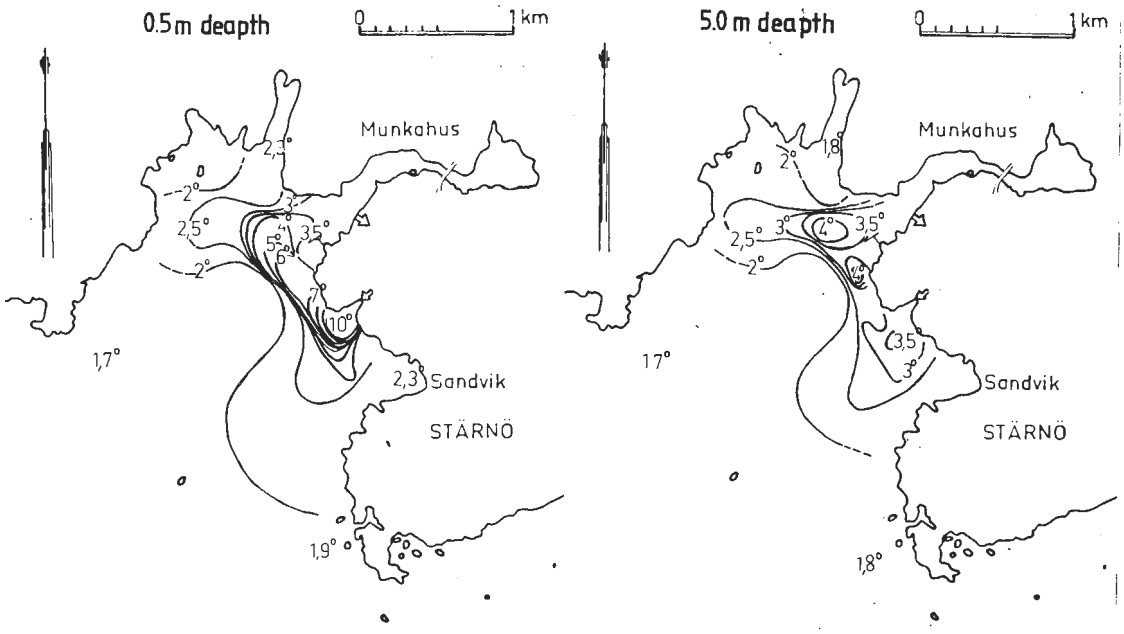

Fig. 4 Sinking cooling water outside Karlshamn Power Plant

Temperature surveys outside the thermal power stations during the winter frequently give as a result another type of temperature pattern. The cooling water is well mixed from the surface to the bottom when the initial jet mixing is finished. An example of such a "plume" is shown in figure 5. The wind was north 11 - 16 m/s and the ambient temperature was 1°C. The waste heat discharged was 49 GWh/day.

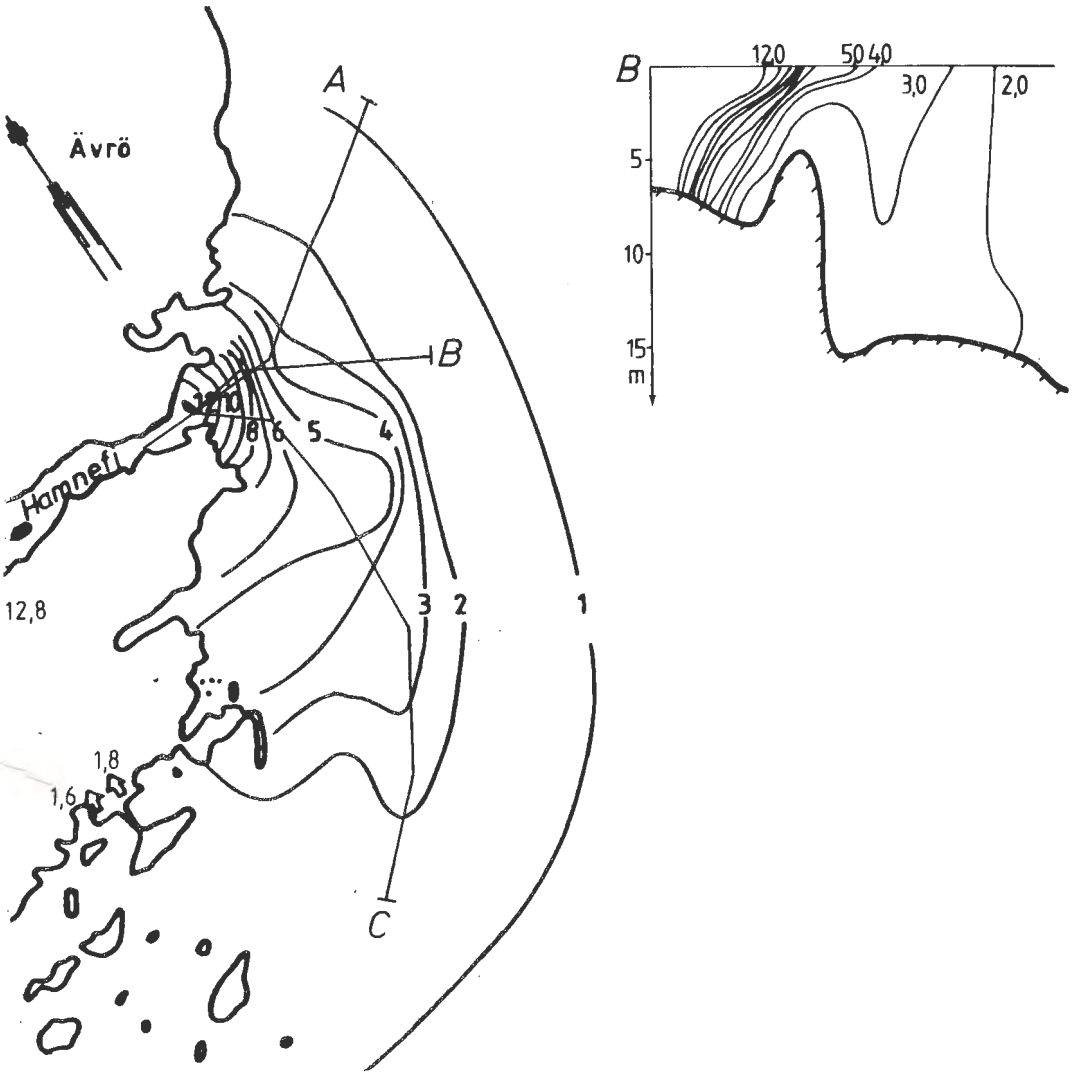

Fig. 5 Example of a sinking plume during rough weather conditions

Another "diving" cooling water plume can be observed when the salinity of the intake water is higher than in the outlet area. The mixed, warm but slightly saltier cooling water is denser than the ambient water and dives below the surface. Normally it finds denser ambient water at a few meters depth and continues to spread at this depth. An example is shown from outside the unclear power station Ringhals at the Swedish West Coast (figure 6).

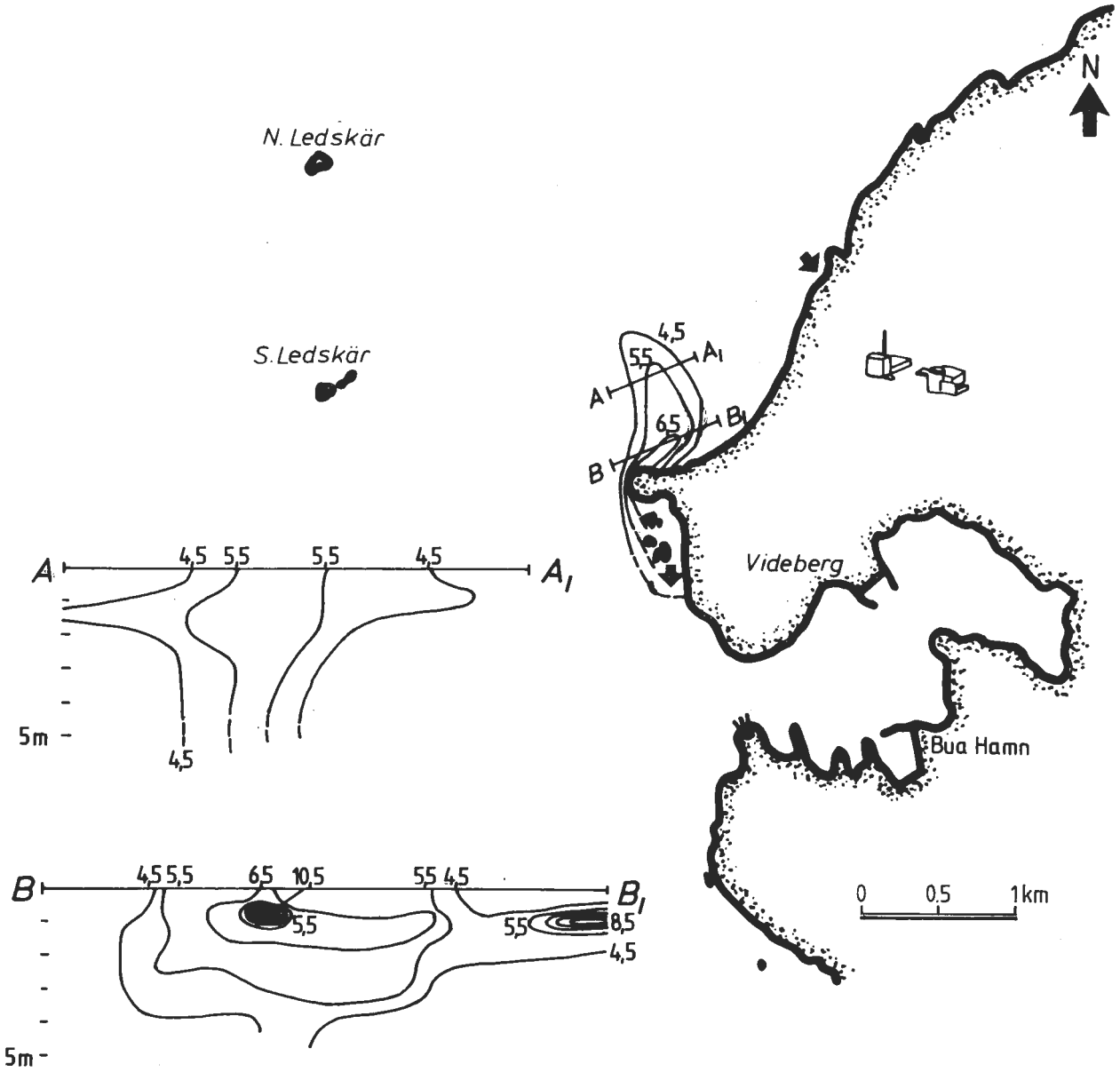

Fig. 6 Sinking due to different density in the intake and outlet area

MODEL EQUATIONS

To make three-dimensional studies of the sinking plume we used a model which was originally developed at the Oceanographic inst. (Inst für Meereskunde), University of Hamburg. The model is fully three-dimensional as opposed to quasi-three-dimensional models or multilayer models. True three-dimensionallity means that the model solves the following set of equations for each grid cell without any integration over layers etc.

$$\frac{\partial u}{\partial t} + u\frac{\partial u}{\partial x} + v\frac{\partial u}{\partial y} + w\frac{\partial u}{\partial z} = -\frac{1}{\rho}\frac{\partial P}{\partial x} + fv + A_D\frac{\partial^2 u}{\partial x^2} + A_S\frac{\partial^2 u}{\partial y^2} + + \frac{\partial}{\partial z}\left[A_V\frac{\partial u}{\partial z}\right]$$

$$\frac{\partial v}{\partial t} + u\frac{\partial v}{\partial x} + v\frac{\partial v}{\partial y} + w\frac{\partial v}{\partial z} = -\frac{1}{\partial}\frac{\partial P}{\partial y} - fu + A_S\frac{\partial^2 v}{\partial x^2} + A_D\frac{\partial^2 v}{\partial y^2} + + \frac{\partial}{\partial z}\left[A_V\frac{\partial v}{\partial z}\right]$$

$$o = -\frac{1}{\rho}\frac{\partial P}{\partial z} - g$$

$$\frac{\partial w}{\partial z} = -\frac{\partial u}{\partial x} - \frac{\partial v}{\partial y}$$

$$\frac{\partial T}{\partial t} + u\frac{\partial T}{\partial x} + v\frac{\partial T}{\partial y} + w\frac{\partial T}{\partial z} = \frac{\partial}{\partial z}\left(K_V\frac{\partial T}{\partial z}\right)$$

$$\rho = \rho(T) = 1.0058 - 8 \cdot 10^{-6}\ (T - 2.5)^2$$

where u, v, w are velocities in the x direction, neg. y-direction and neg. z-direction.

ρ is density, f is the coriolis parameter

A_D is the eddy viscosity coefficient for terms of the type

$\frac{\partial^2 u}{\partial x^2} + \frac{\partial^2 v}{\partial y^2}$ (divergence)

A_S is the eddy viscosity coefficient for terms of the type

$\frac{\partial^2 u}{\partial y^2} + \frac{\partial^2 v}{\partial x^2}$ (shear)

A_V is a variable vertical eddy viscosity coefficient.

K_V is a vertical eddy diffusivity coefficient.

P is pressure
t is time
T is temperature

It is assumed that heating due to compression or cooling due to expansion is negligible. The so called adiabatic temperature changes is thus not taken into account. The model is intended to be used for convection problems in shallow (depth < 50 m) water and is not to be used in deep ocean where the adiabatic temperature changes can be of importance.

The density is everywhere very close to the value = 1.0000 g/cm^3. The deviation $\Delta\rho$ is therefore omitted in the intertia terms. It is of primary importance in the buoyancy term. Neglecting $\Delta\rho$ in the intertia term is the so called Boussinesq approximation. Phillips (1966) showed that it is also valid when treating convection problems.

The turbulent heat and momentum exchange are modelled using eddy viscosities and turbulent heat conduction coefficients. The dependens of these coefficients on grid spacing, density and velocity gradients will be discussed in sections "HORIZONTAL MIXING" and "VERTIKAL MIXING".

MODEL FRAMEWORK

The grid

To study a heated water plume a model with high resolution is needed. The very strong temperature and velocity gradients in the plume must be adequately represented, or the computed mixing will be wrong. On the other hand the model must include areas of water, which is not influenced by the heated water at all. This leads to a grid, where the gridsize is changing in space. In the plume the gridsize is small, and close to the boundaries a bigger gridsize is used (figure 7).

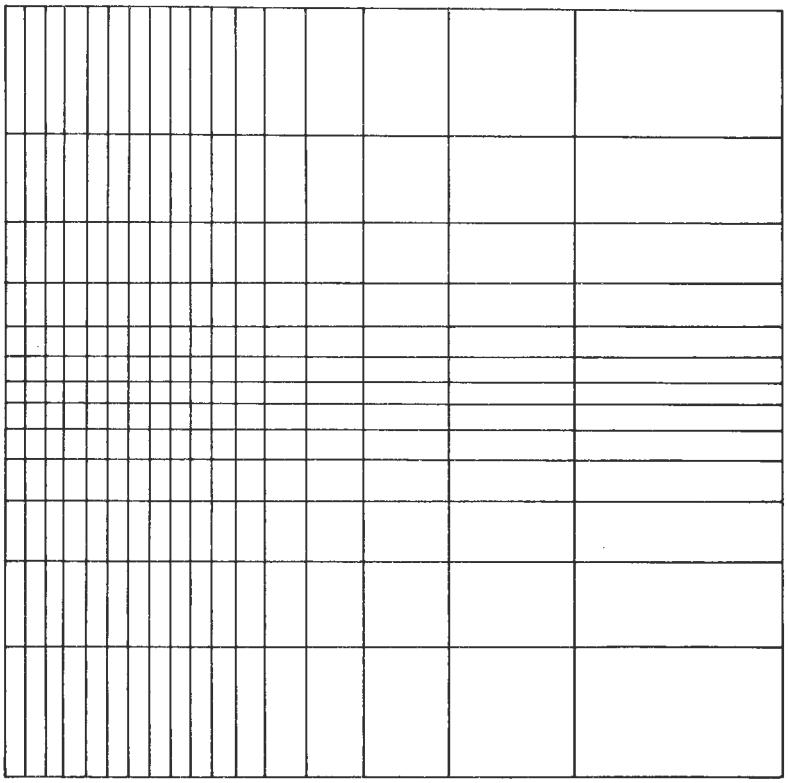

Fig. 7 An example of a mesh with variable gridsize.

The grid is staggered. The indexing is done in the following way:

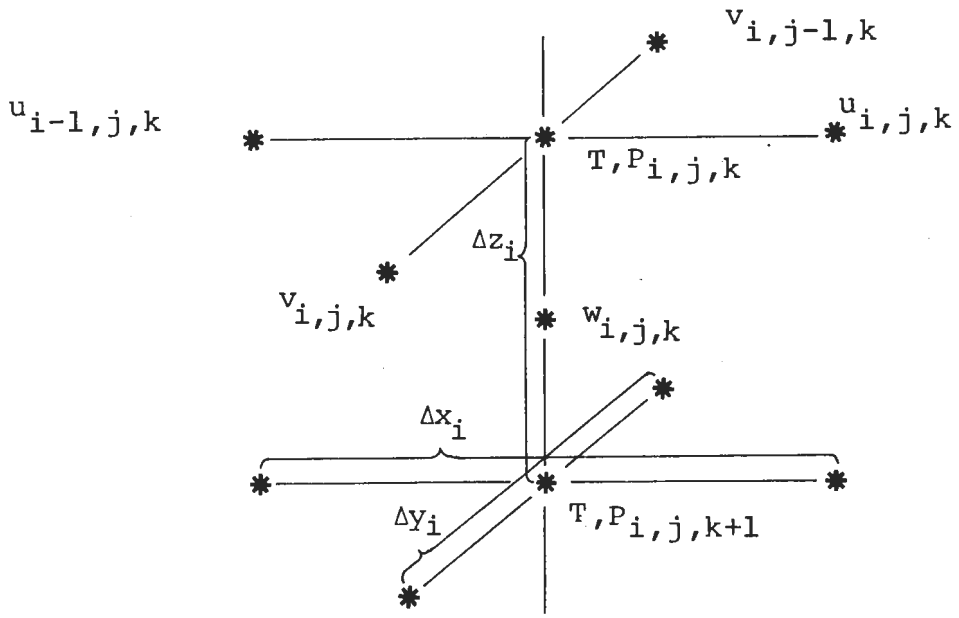

The surface lies between $u_{k=2}$ and an artificial $u_{k=1}$, the undisturbed surface, $z = 0$, being defined at the level of $w_{k=1}$.

The bottom is taken into account by prescribing the depths in the pressure points (h_p) and calculating the depths in the velocity points (h_u, h_v).

$$h_u = \min \left[h_p(x + \frac{\Delta x}{2}), h_p(x - \frac{\Delta x}{2}) \right]$$

$$h_v = \min \left[h_p(y + \frac{\Delta y}{2}), h_p(y - \frac{\Delta y}{2}) \right]$$

u, v, T are calculated only where the depth of the calculation level is less than h_u, h_v, h_p respectively.

Boundary conditions

The prescribed condition at the boundaries of the model is very important. Bottom stress, heat loss to the atmosphere, wind stress etc. are examples of boundary conditions.

Using a stretched grid the open boundaries are that far from the outlet that all transports can be assumed to be out of the area under consideration, and the velocity to be small. The upwind scheme used for advection does not need any boundary conditions in this case. The error made by using u, v, = 0 as boundary values for the viscous terms is negligible.

There is in the model no explicit diffusion of temperature, unless for unstable density stratification. That is because using upwind differences is accompanied by numerical diffusion of the order of $K = \frac{u\Delta x}{2}(1 - \frac{u\Delta t}{\Delta x})$ or $K \approx \frac{1}{2} u\Delta x$ (Roache 1972). For the pressure term the water level at the boundary is prescribed.

The bottom boundary condition for temperature is: No diffusion, no advection through the bottom. The condition at the surface is the same. In an earlier study of sinking plumes (Bork 1978) is shown that the heat loss to the atmosphere does not change the picture of the sinking plume to any extent. There are two reasons to support this result. 1) The plume area exposed to the atmosphere is small compared with a floating plume. 2) Sinking plumes occur at fairly weak winds. The heat loss is thus smaller than in the average case. The heat loss to the atmosphere is thus neglected in this study.

At the bottom and at the side walls a no slip condition is used.

Wind influenced currents are not studied in this report. Wind stress is therefore equal to zero.

Salinity is introduced in the model for the only reason of controlling the change of the density with temperature. No salt sinks or sources exist in the model and the salinity is everywhere 8 $^{o}/oo$, which is a probable value for winter conditions in the central Baltic from the surface down to about 30 m at least.

The boundary conditions at the power plant outlet are as follows. In a 50 m wide and 2 m deep open section in the coastline water is flouting out at a rate of 36 m^3/s. The water is 11 ^{o}C. The model boundary condition tries to simulate the opening of the narrow fjord Hamnefjärden (see map figure 18). The real outlet is situated on the south shore of that fjord. However, heated water is most of the time fully mixed inside the little fjord and is going out into the Baltic as a surface flow of a two layer flow at the mouth of the fjord.

Horizontal mixing

For the horizontal mixing of momentum two coefficients are introduced in this model. One A_{SHEAR} for the terms of type $\frac{\partial}{\partial y}(A \frac{\partial u}{\partial y})$, where u is the velocity perpendicular to the y-direction. The other A_{DIV} for the terms of type $\frac{\partial}{\partial y}(A \frac{\partial v}{\partial y})$, where v is parallell to the y-direction. There is a possibility in the model to use different values for A_{SHEAR} and A_{DIV}. In this study no serious tests have been carried through to conclude the importance of this. In most of the runs $A_{SHEAR} = A_{DIV} = \text{Const} = 0.04$.

The two constant coefficients A_{SHEAR} and A_{DIV} define in the model the value of the horizontal eddy viscosity through the formula

$$A_{SHEAR} = \frac{\Delta t \cdot A_H}{\Delta L_{min}^2},$$

where A_H is a variable horizontal eddy diffusion coefficient, Δt is the time step and ΔL_{min} is the minimum grid size at the grid cell under consideration. For $\Delta t = 20$ sec $\Delta L = 50$ m in the central part of the plume the formula gives

$$A_H = \frac{A_{SHEAR} \cdot \Delta L^2_{min}}{\Delta t} = 5 \text{ m}^2/\text{s}.$$

The reasoning behind this is that turbulence (which causes the diffusion) is the motion of time scales shorter than Δt, the time step in the model. It can also be said that it is the motion whith length scale less than the smallest grid size at the grid cell under consideration. If the time step is changed, the turbulence gets another definition-time scale, which in this case is taken into account in the formula. More important is that if you have a stretched grid, it can be argued that turbulence has different definitions at different locations in the model. In the very large grid cells at the outer corners in the model "turbulence" is small eddies up to rather large movements. In small cells near the outlet "turbulence" is only the small eddies. This is also accounted for in the formula.

In the present study this facility is used with cautiousness. The grid size in the central part of the model, where the plume mixes with the surrounding water, the grid is kept constant 50 x 50 m. Further out, where the velocity gradients are small, the grid size is allowed to grow rapidly. The reason for the hesitation to use the formula in the central, important region is the following example given by Nihoul (1975) and also tests with the model with different time steps.

In a tidal model of the North Sea, turbulence can be defined as the motion with time scale less than 5 min. A length scale to be associated with this time scale can be computed with the formula

$$l \sim \varepsilon^{1/2} \cdot t^{3/2}, \text{ where } \varepsilon \approx 10^7 \text{ m}^2/\text{s}^3.$$

The associated length scale is 5 m. The action of turbulent eddies smaller than 5 m will then be described via an eddy viscosity term. However, the grid size of a model for the North Sea must be much bigger, typically of the order of 5 km. The caracteristic time associated with scales of motion of the order of a few kilometers is of the order of a day. This is of course too big a time-step to be used in a numerical model of this kind.

In a test with the sinking plume model, where the time-step Δt was 10 sec instead of the "normal" 20 sec, it was shown that the plume was much wider and smoother than in the "normal" case. This was obviously depending on the mixing, which in this test run was doubelled by the formula $A_{SHEAR} = \frac{\Delta t \cdot A_H}{\Delta L^2 min}$.

Vertical mixing

The vertical eddy viscosity is dependent on the stability and on the velocity gradient.

$$A_V = A/\left(1 + 10\ \frac{\Delta\rho}{\Delta z}/\left(\frac{\Delta v}{\Delta z}\right)^2\right)^{1/2}.$$

The formula is found for example in Munk, Anderson (1948).

If $\Delta\rho/\Delta z > 0$ (unstable conditions) the formula is not recommended or tested. In unstable conditions $A_V = A$ in the model.

The behaviour of the plume is very dependent on the value of A. This dependence is discussed later in the "result" section.

The vertical mixing in the coastal area studied is probably wind (wave) generated. No other strong sources like strong velocity gradients exist (not even in the plume itself). A formula for the wind generated turbulence can be found in U Svensson (1979). The vertical eddy viscosity is given as a function of wind velocity and depth. In wind speeds less than 5 m/s the value is fairly constant from 1 m below the surface down to at least 10 m. The eddy viscosity coefficient proposed is $A = 0.026 \cdot v_*^2/f$, where v_* is the surface friction velocity. f is the Coriolis parameter. This formula is later on used to relate the mixing to a wind velocity. There is in the model no explicit temperature diffusion. K_V is zero for most of the time. Only if the density stratification is unstable, it is $K_V = 0.2 \cdot t/\Delta\rho/\Delta z^2$, where t is time and 0.2t is limited to 1000.

RESULTS

Flat bottom

The first tests at the SMHI with a model of sinking plumes were performed in a two dimensional model (one horizontal dimension, one vertical dimension) by I Bork (1978). It was from the beginning concluded that a fully three dimensional model was needed to describe a real sinking plume. However, many valuable tests could be conducted with a two dimensional model. A heated water plume is a three dimensional problem by its own nature. It is important to describe velocity, spreading and mixing in the along-axis direction, the spreading and mixing in the direction perpendicular to the axes of the plume and finally the mixing and in this study also sinking of the plume in the vertical direction. Moreover the coastline and bottom topography near the cooling water outlet almost always play an important role in the plume movements. The topography also needs a three dimensional description.

A series of tests in the present study was carried out in a model with a gently sloping bottom outside the cooling water outlet and further out a flat bottom at 14 m depth. The horizontal eddy viscosity coefficient can be estimated with the theory of Kolmogorov (Nihoul, 1975): $A = \varepsilon^{1/3} l^{4/3}$, where E is the rate of energy transfer between eddies of different scales. L is the length scale of the turbulent eddies.

If the turbulent length scale in the model is $\approx$ 50 m = smallest grid size, ε is about 10^{-6} to 10^{-8} m^2/s^3. The horizontal eddy viscosity coefficient is then of the order of magnitude: $0.4 < A_H < 2$ m^2/s. Two tests were carried out. One with $A_H = 0.5$ m^2/s and the other with $A_H = 5$ m^2/s.

The result shows that the plume in the first case is narrow with the high velocity reaching far out. The very small horizontal mixing does not, however, produce a totally unrealistic plume. The sinking took place further out from the outlet compared to the second run, but neither the sinking velocity nor the temperature at the bottom was significantly altered by the 10-fold change in horizontal mixing. It is concluded that the model is not very sensitive to changes in the horizontal eddy viscosity coefficient. The coefficient used during the following tests is 5 m^2/s.

The vertical eddy viscosity coefficient is very important for the result. The vertical turbulence in the area is presumably caused by wind (wave) mixing. One estimate of the wind introduced vertical eddy viscosity coefficient is given by U Svensson (1979).

$$A_V = 0.026 \cdot v_*^2/f$$

$$f = 1.25 \cdot 10^{-4}\ s^{-1}$$

$$v_* = \sqrt{\frac{\tau}{\rho}} = \sqrt{\frac{3.2 \cdot 10^{-6} \cdot W^2}{1}}\ cm^2/s,$$

where W is wind velocity in cm/s. A wind velocity of 400 cm/s gives $A_V \sim 100\ cm^2/s = 0.01\ m^2/s$.

Wind velocities between 1 and 1.5 m/s produce an eddy viscosity coefficient = 0.001 m^2/s. In the model test first carried out with the intension to study vertical mixing the coefficient was 0.01 m^2/s. This resulted in a plume, where the downward velocity in the front of the plume was rather weak (0.1 cm/s). The cooling water mixes down to the bottom at 14 m, and no pronounced vertical temperature gradient exists. The horizontal temperature gradient is more or less like a vertical wall separating the mixed cooling water from the ambient 0^o water. The situation in the model is similar to the most common observed situation described earlier. From the model studies it is concluded that this

situation occurs, if the wind velocity is more than 4 m/s, the equivalent of horizontal eddy viscosity greater than 0.01 m^2/s.

The next situation studied was an identical case with the vertical eddy viscosity coefficient equal to 0.001 m^2/s (one tenth of the earlier used value). The result changed to a situation comparable to observed situations described earlier with weak winds. The run was like all the others started from zero. The ambient current was 0 cm/s, the temperature was 0 ^{o}C. At time 0 h the pumping started of 0 ^{o}C water through the outlet. After ≈ 2 hours, outlet of the heated water of 11 ^{o}C started.

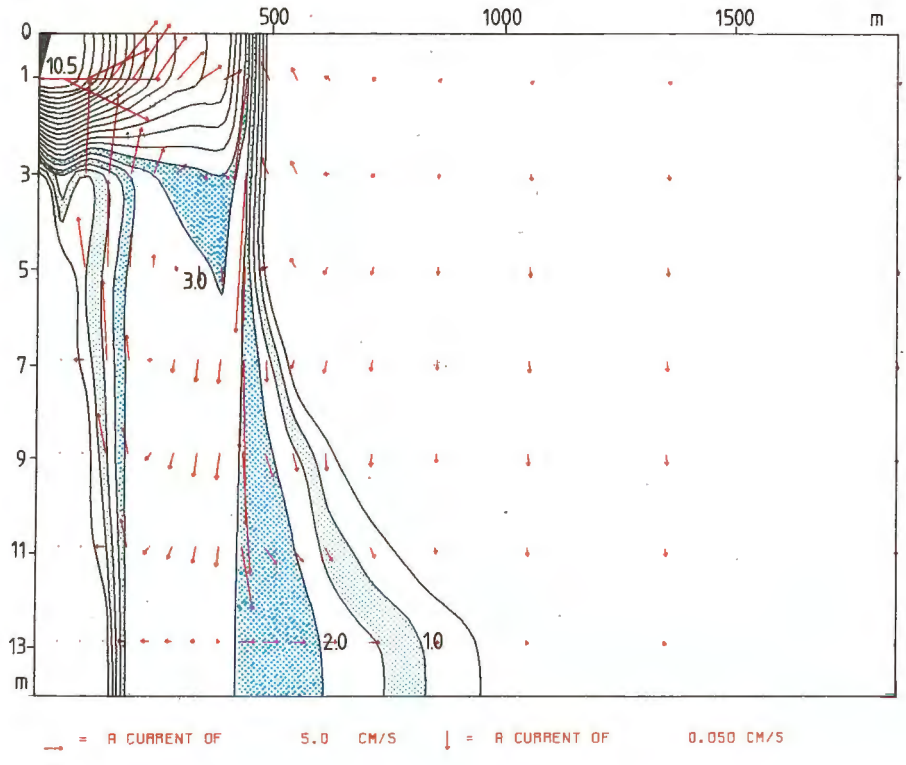

Fig. 8 A section out from the coast. (centerline)

The run was continued for 11 hours totally. At that time a quasi-steady state had been reached. The plume continued to spread along the bottom with velocities of 1 - 5 cm/s, but the temperature and the velocities in the sinking region (450 - 500 m from the shore) were not changing significantly with time. Figures 8 to 12 show different views of the plume after 11 hours from start. The sinking velocities are much higher than in the earlier case.

During the development of the plume as high vertical velocities as ~0.7 cm/s were computed. The maximum computed temperature at the bottom was 3.1 °C. This is about 0.5 °C higher than the temperature for maximum density for water with the salinity 8 °/oo. The sinking water around the high temperature core has a temperature around the temperature for maximum density. The warm water core, which is only a little lighter than the surrounding, is probably dragged down by the action of the sinking around.

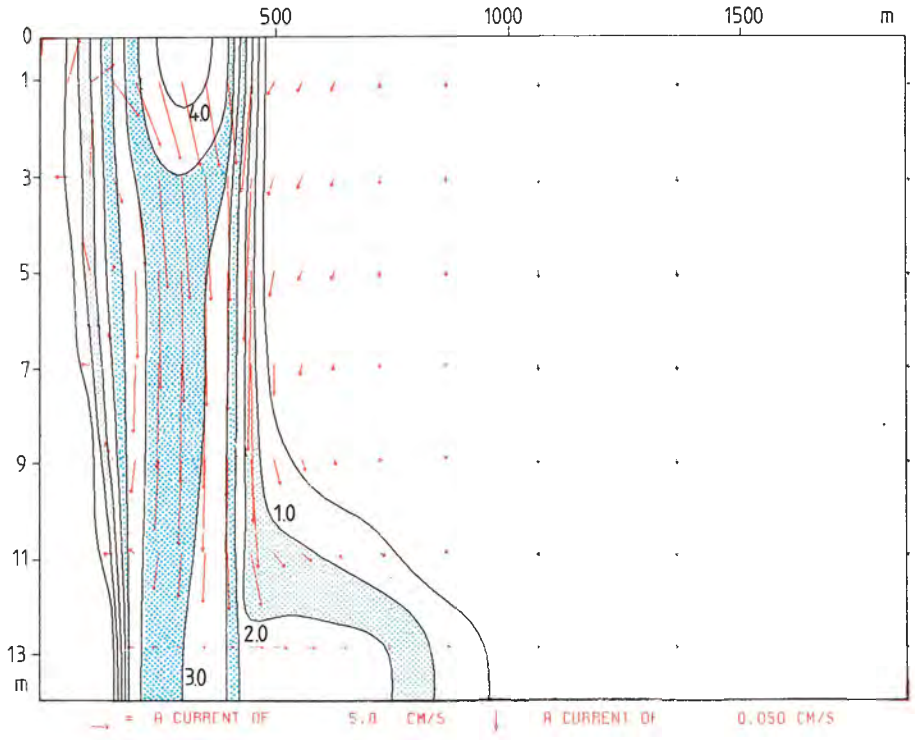

Fig. 9 A section out from the coast. (100 m north of the outlet)

It is seen from figure 10 that the sinking does not only take place in front of the plume but at all boundaries, where cooling water meets the ambient water. The highest vertical velocities and the highest bottom temperatures are, however, found at the outer edge of the plume.

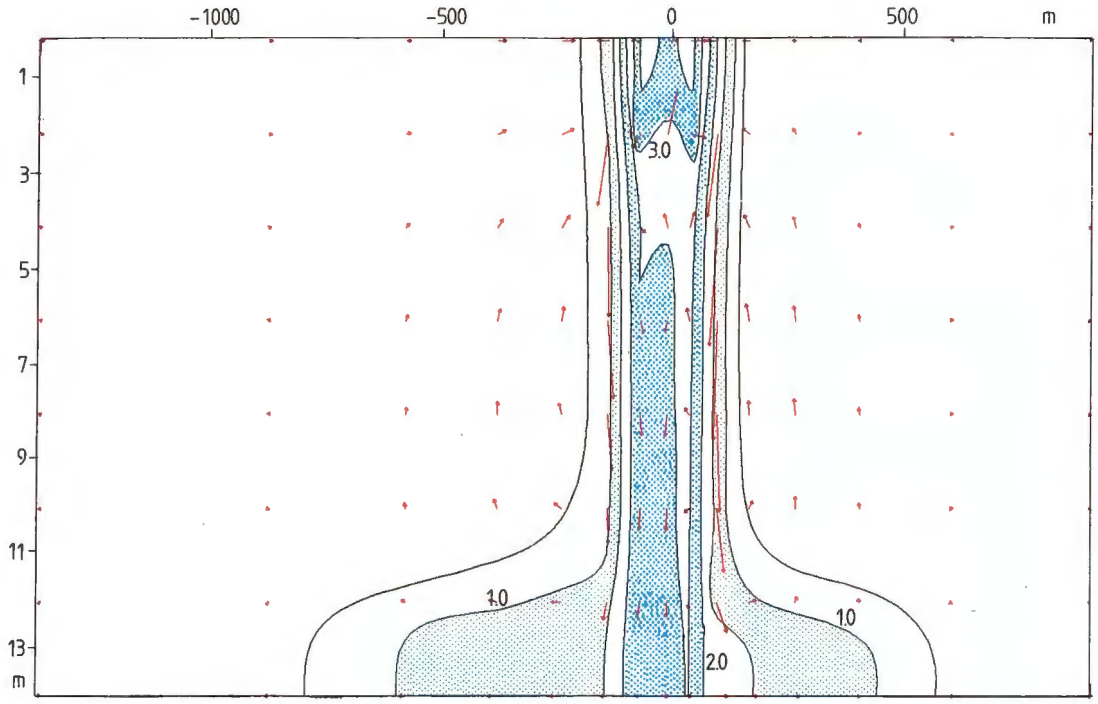

Fig. 10 A section along the coast 400 m from the shoreline.

Next a really small vertical eddy viscosity was used $A_v = 0.0001\ m^2/s$. Theoretically this coefficient can be valid for very low wind velocities, less than 0.5 m/s. The result is very like the case where $A_v = 0.001$. The plume is of course not so wide and is reaching 50 m

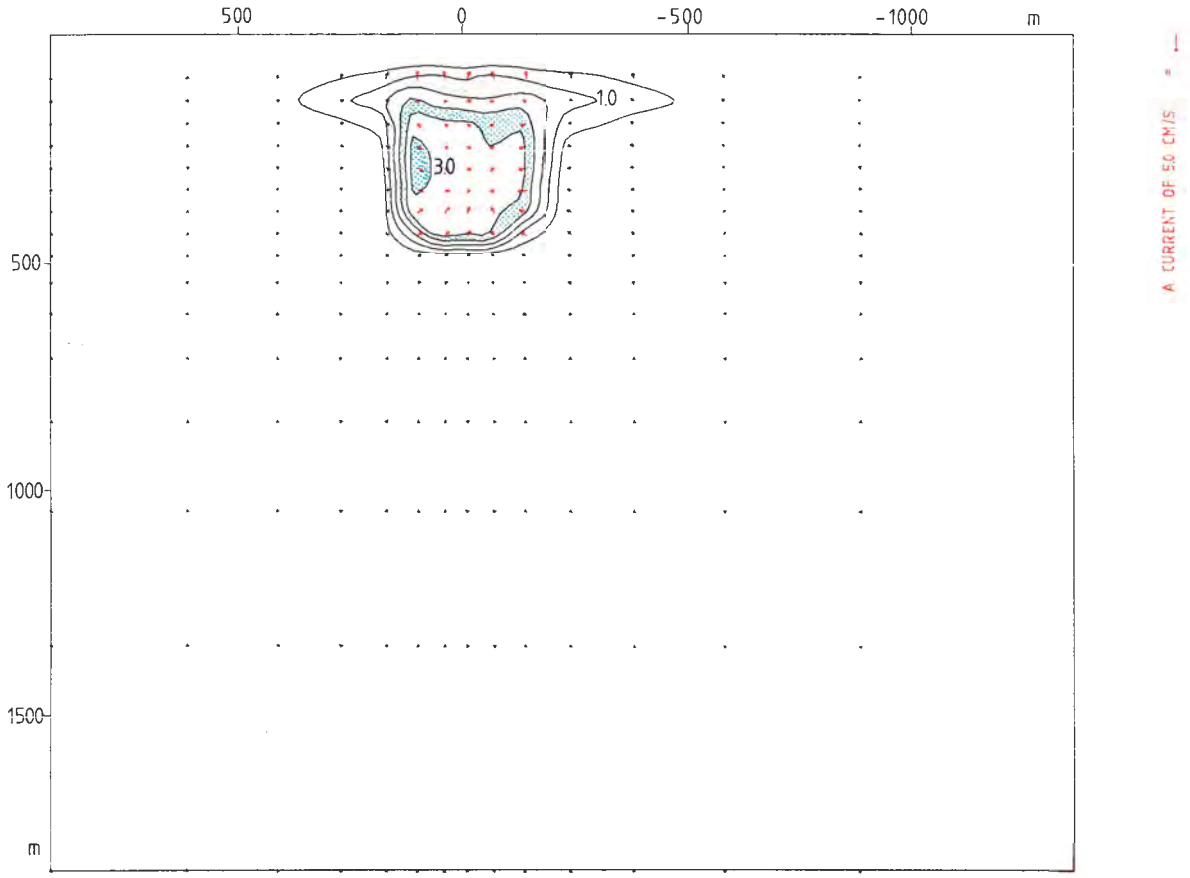

Fig. 11 The plume at 6 m depth.

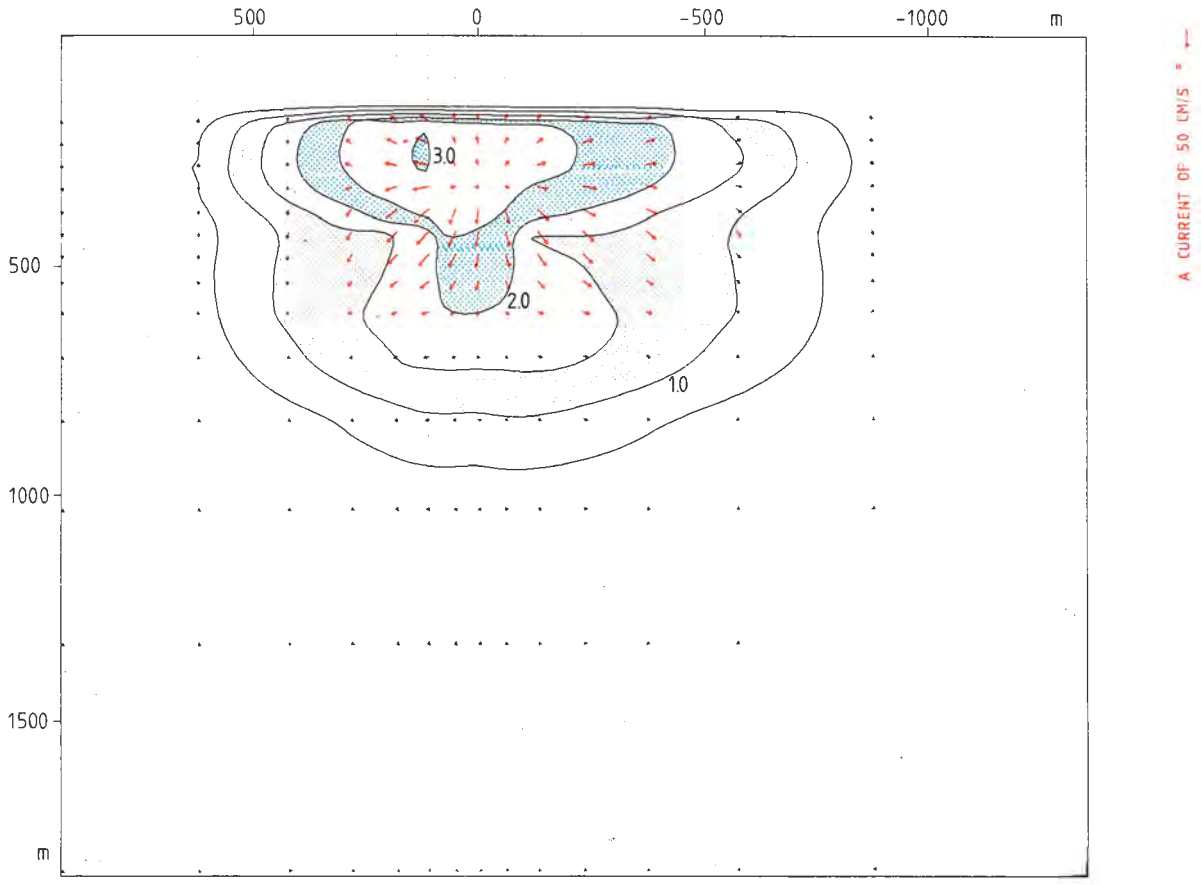

Fig. 12 The plume at the bottom.

further out at the surface due to reduced friction. The sinking velocity and the temperature computed at the bottom has not changed. The reason is that the mixture of cooling water and ambient water is the same (maximal density) in the sinking region in the two cases. During the sinking the downward velocity is not affected by the vertical eddy viscosity but more by the horizontal eddy viscosity.

The next step was therefore to reduce also the horizontal eddy viscosity by a factor of 10 A_h = 0.5 m^2/s, A_v = 0.0001 m^2/s. This resulted in an unrealistically narrow surface plume, which was, after sinking, spreading rapidly at the bottom. The only interesting result was that the sinking, which was expected to be rapid, instead was computed to be slower than before. The sinking core was namely so narrow that the ambient water, despite of the small horizontal mixing coefficient, was able to slow down the sinking water. The density driven sinking was therefore small compared to the earlier cases. The result is probably somewhat distorted by numerical diffusion of temperature and momentum, as the plume is not more than 3 grid points (150 m) wide. The numerical diffusion is, however, not larger than that you can see a marked difference between the cases with A_h = 0.5 and A_h = 5.

The conclusion drawn by the sets of runs is that the sinking, although dependent on especially the vertical eddy viscosity, does not increase, as the eddy viscosity gets very small but reaches a maximum for A_v = order of magnitude 0.001.

Artificial bottom topography

Before real bottom topography was introduced in the model one run was made with a long ridge at the flat bottom. The ridge goes along the straight coastline about 350 m out from the coast. It rises 5 m from the bottom which is at 14 m depth. The ridge was placed in this position so that the sinking should occur at the seaward slope. The intention was to study if the slope would act to increase the sinking of the plume. The eddy viscosity coefficients were A_h = 5 m^2/s, A_v = 0.001 m^2/s as in the run shown in figures 8 to 12.

The case with the artificial bottom topography was started from zero. That is, the temperature was everywhere 0°C and the velocities were 0 cm/s. At time equals zero the pumping of 0°C water from the outlet starts. After 2 hours the heated water (11°C) was turned on. The study was continued for 14 hours totally.

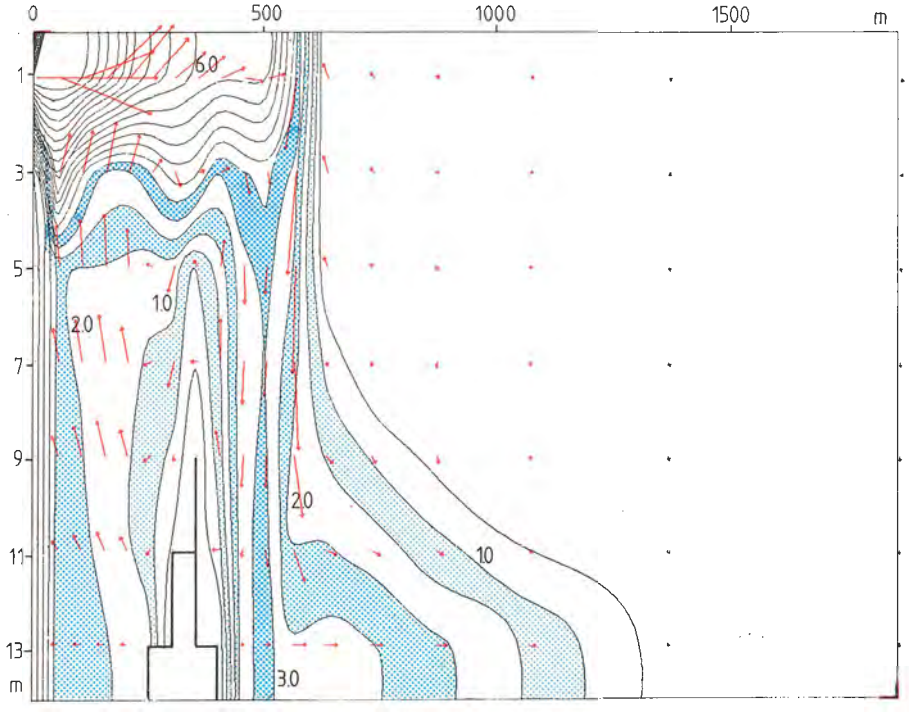

Fig. 13 A section out from the coast. (centerline)

— = A CURRENT OF 5.0 CM/S | = A CURRENT OF 0.050 CM/S

Over the ridge the warm water flows as an upper layer below which a weak undercurrent takes colder water towards the coast. Most of the cold water that mixes into the plume however comes from the sides. This is shown in figures 13, 14 and in figure 16 below.

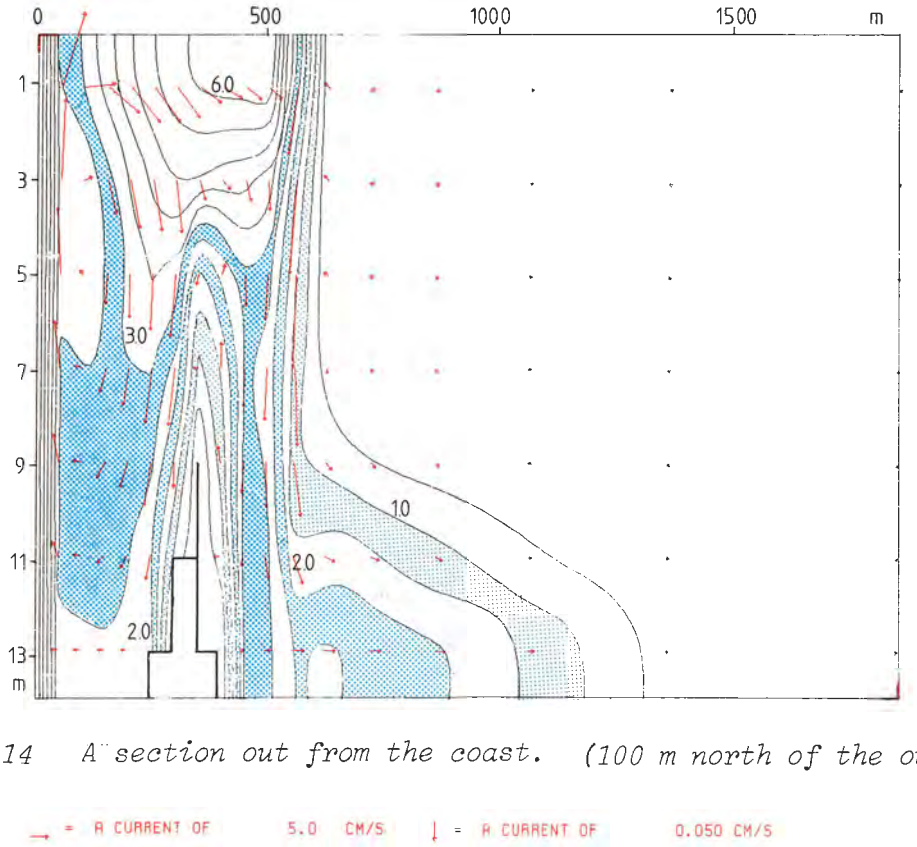

Fig. 14 A section out from the coast. (100 m north of the outlet)

Right outside the outlet the plume, because of its relative high velocity (37 cm/s) mixes with the underlying cold water. It thereby gets thicker and wider (see figures 13 and 16). After ≈ 100 m the buoyancy seems to be the most important spreading force. The plume from 100 m to 300 m gets thinner and wider. Cold water intrusion from below is still taking place especially in the center of the plume, where the horizontal velocity is high (figures 13 and 15).

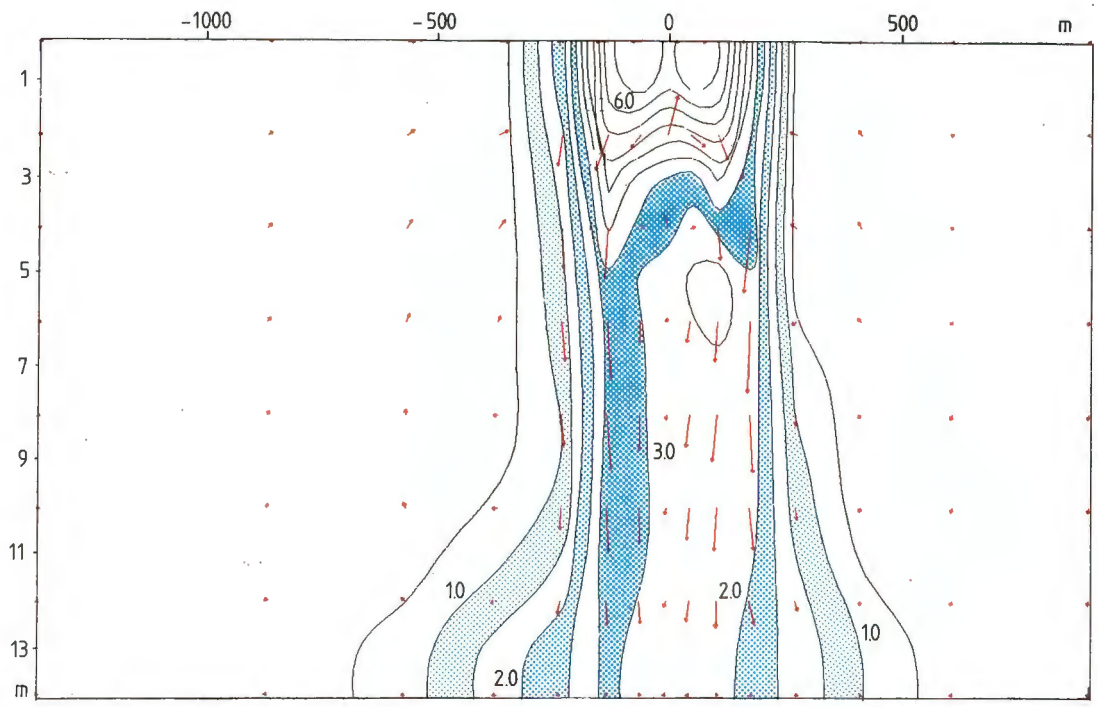

Fig. 15 A section along the coast 450 m from the shoreline.

At 350 - 400 m from the outlet the mixture of cooling water and the ambient water has reached the temperature for maximal density and the water here starts to sink. Outside the sinking zone the surface current is directed towards land (figures 13 and 16). Sinking also takes place 50 to 150 m on both sides of the centerline of the plume, where cooling water and ambient water forms a maximal density mixture (figures 15 and 16). The most rapid sinking and the highest bottom temperatures are computed in front of the plume (figures 13 and 17). At the bottom the dense 2 - 3^{o}C water continues to spread in a 3 - 4 m thick layer.

What is described above is not only valid for the case with the artificial bottom topography but is described here in connection to the figures for that case.

Comparison between the two runs, where the only difference is the bottom topography, shows that the slope in the run in figures 13 to 17 increase the sinking somewhat. Vertical velocities in the two cases are about the same (max 0.6 - - 0.7 cm/s). The temperature at the bottom is during the development of the topography case as high as 3.3°C, which is 0.2°C higher than without bottom topography. If this small difference is due to a small acceleration of the vertical flow or a blocking of the horizontal flow is not clear. The suspicion is, however, that the most important effect is just the blocking of the horizontal flow at the bottom. The sinking water can only flow seawards and can not be sucked landwards and into the outgoing plume.

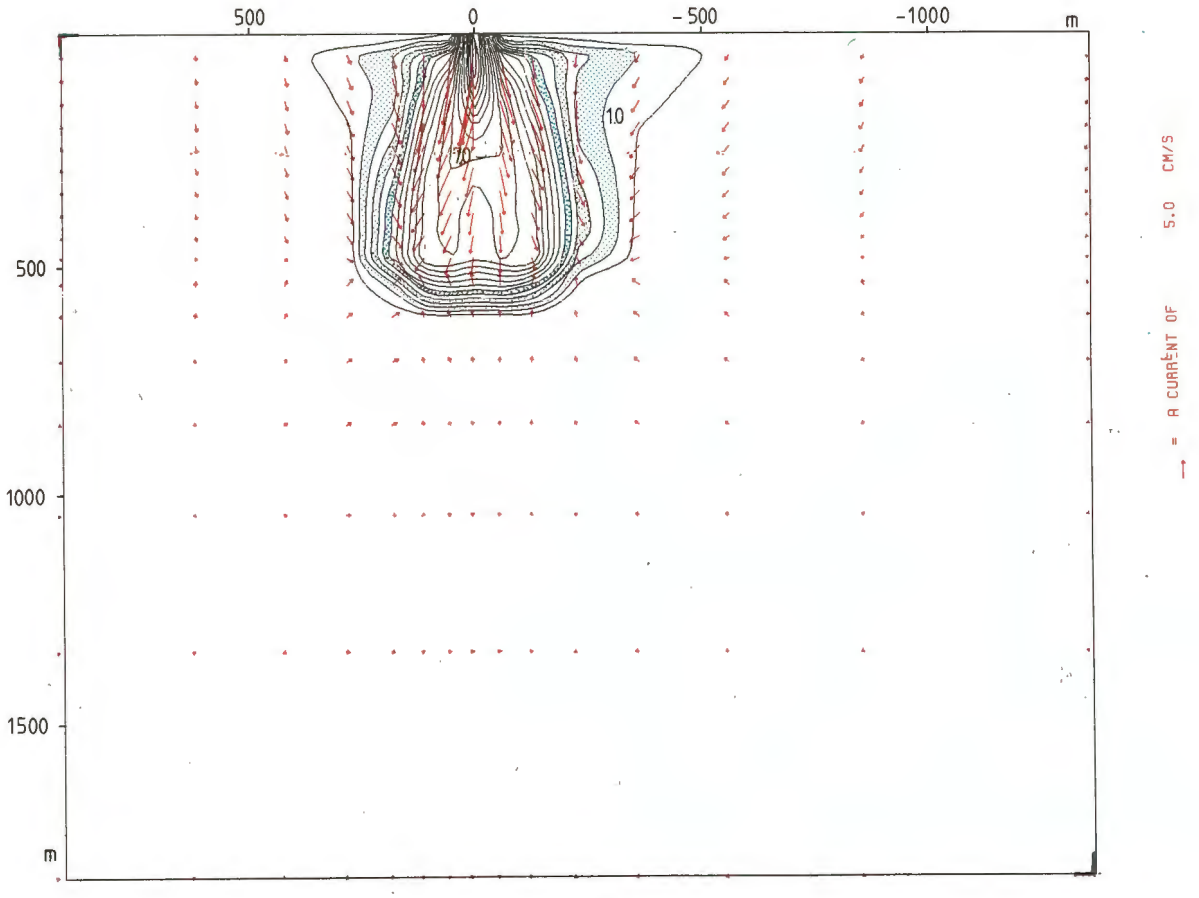

Fig. 16 The plume at the surface.

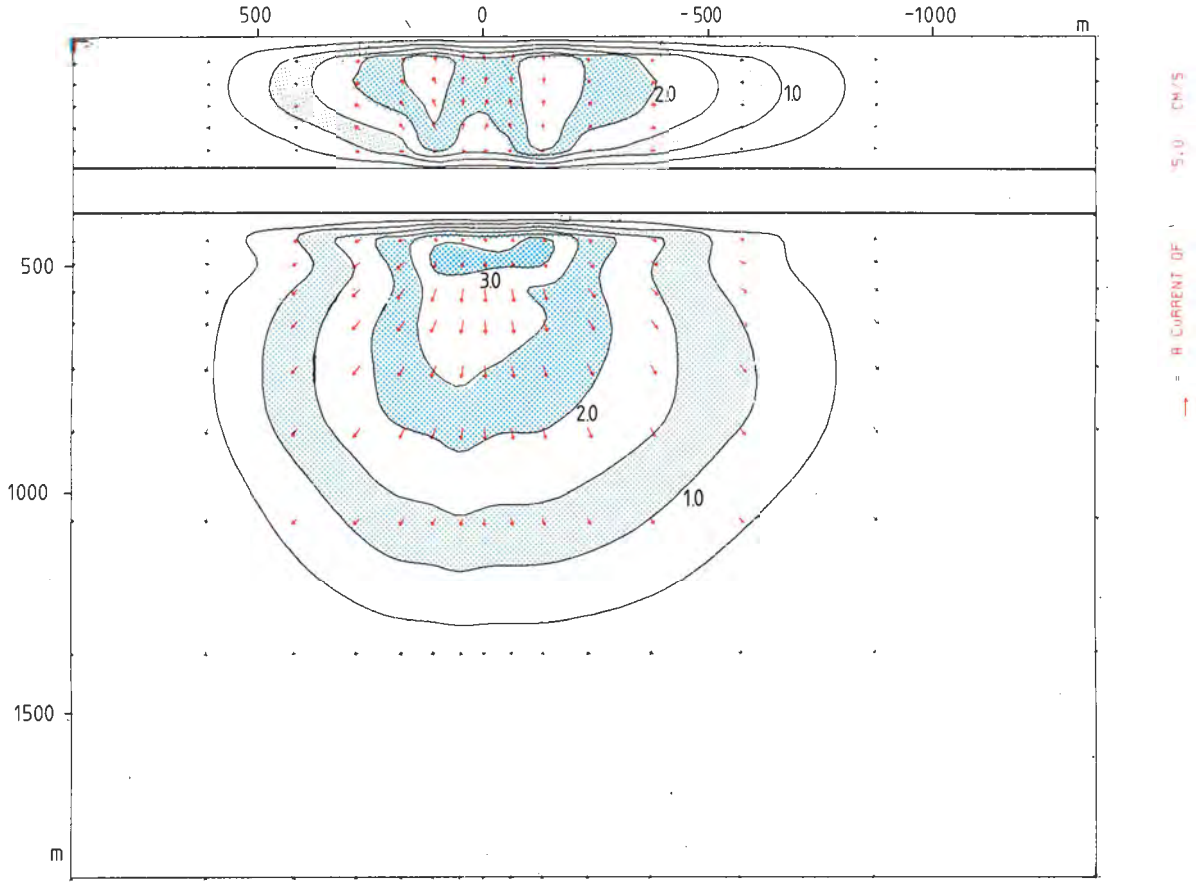

Fig. 17 The plume at the bottom.

Bottom topography of the Simpevarp area

The heated water from the nuclear power plant at Simpevarp north of Oskarshamn is ejected in a small fjord. In the mouth of the fjord the heated water is entering the Baltic as an outgoing surface layer. The coast is rather ragged with small bays and skerries. The 10 m depth line goes, however, close to the coast, so that the outlet is in relatively deep water, as can be seen from the navigational chart (figure 18).

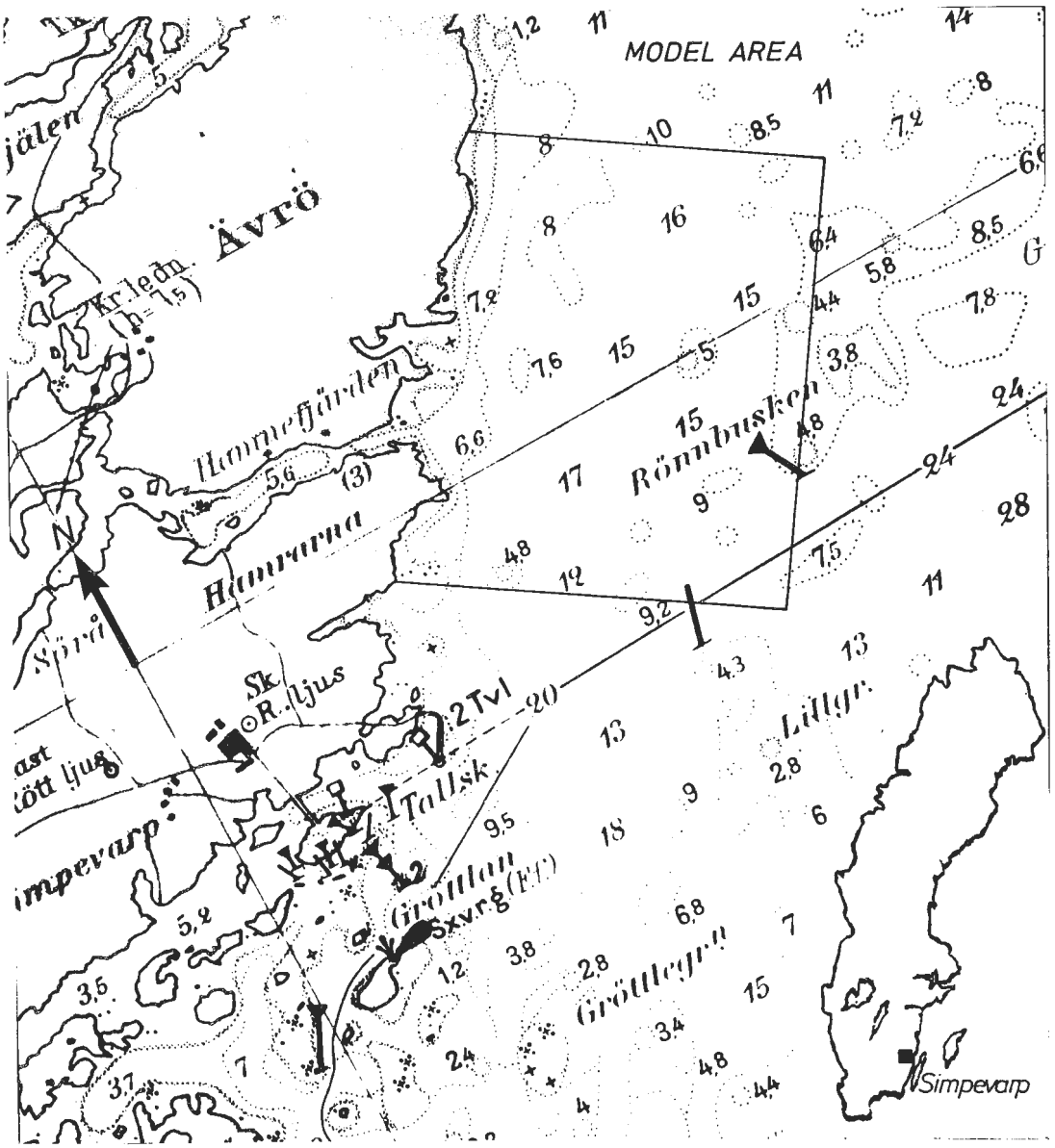

Fig. 18 Bottom topography of the Simpevarp area.

An area with shallow water ≈1 km from the coast prevents deep water to flow eastward. This shallow ridge is just outside the east boundary of the model but is included in the model topography as a shallow outer boundary. In figure 19 a more detailed depth chart is shown together with the model view of the bottom topography.

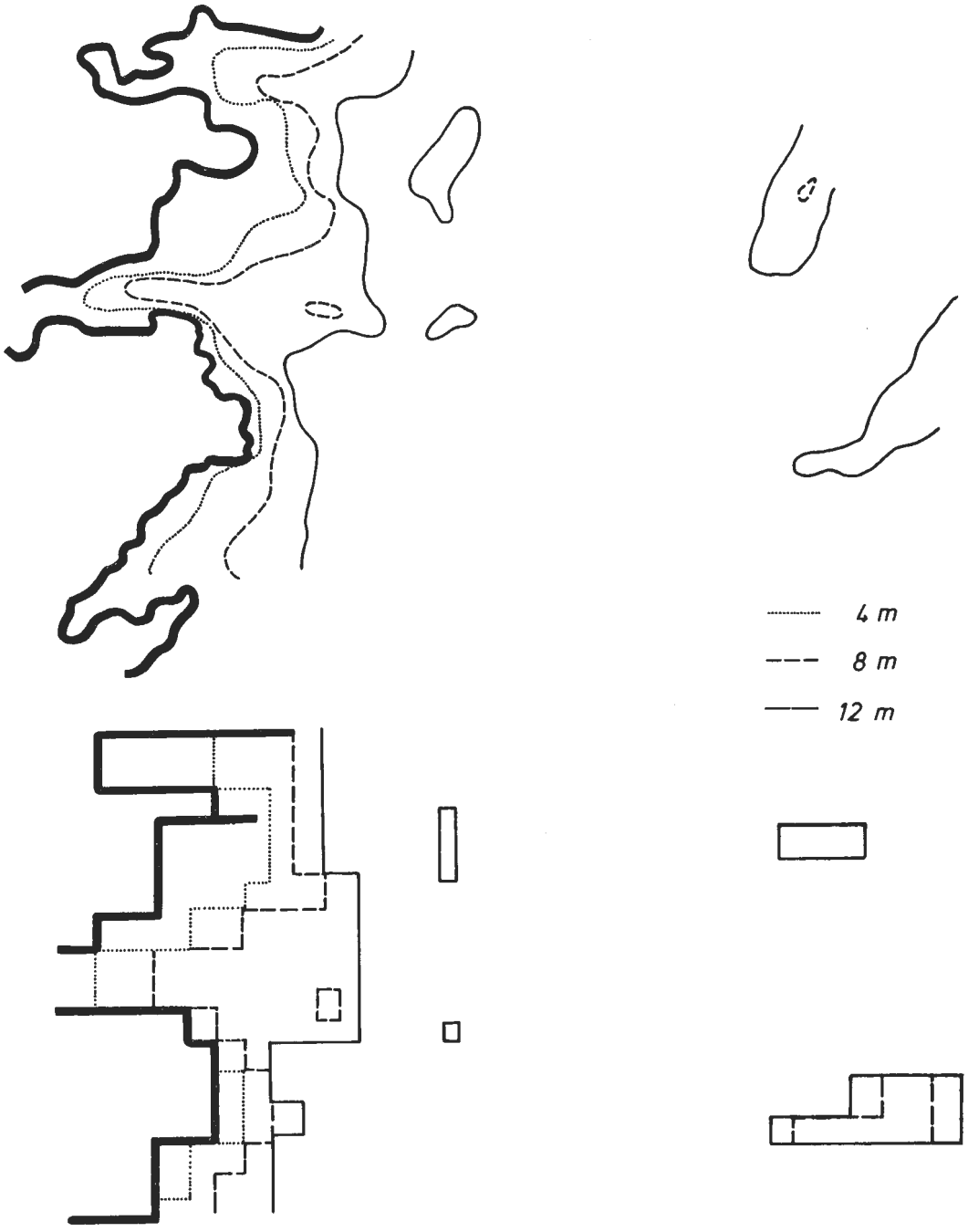

Fig. 19 Detailed depth chart and model view of the bottom topography.

The run with real bottom topography was again started from rest with 0°C water of 8 °/oo salinity in the Baltic. After 2 hours of pumping 0°C water the heated water was turned on. The mixing coefficients had the same values as those in the run with artificial topography, e.g. the vertical eddy viscosity equals 0.001 m^2/s. The horizontal eddy viscosity coefficient $A_H = \frac{0.04 \cdot \Delta L^2 \text{ min}}{\Delta t}$, where ΔL min is the smallest horizontal grid length in the cell under consideration, and Δt is the time step (= 20 s).

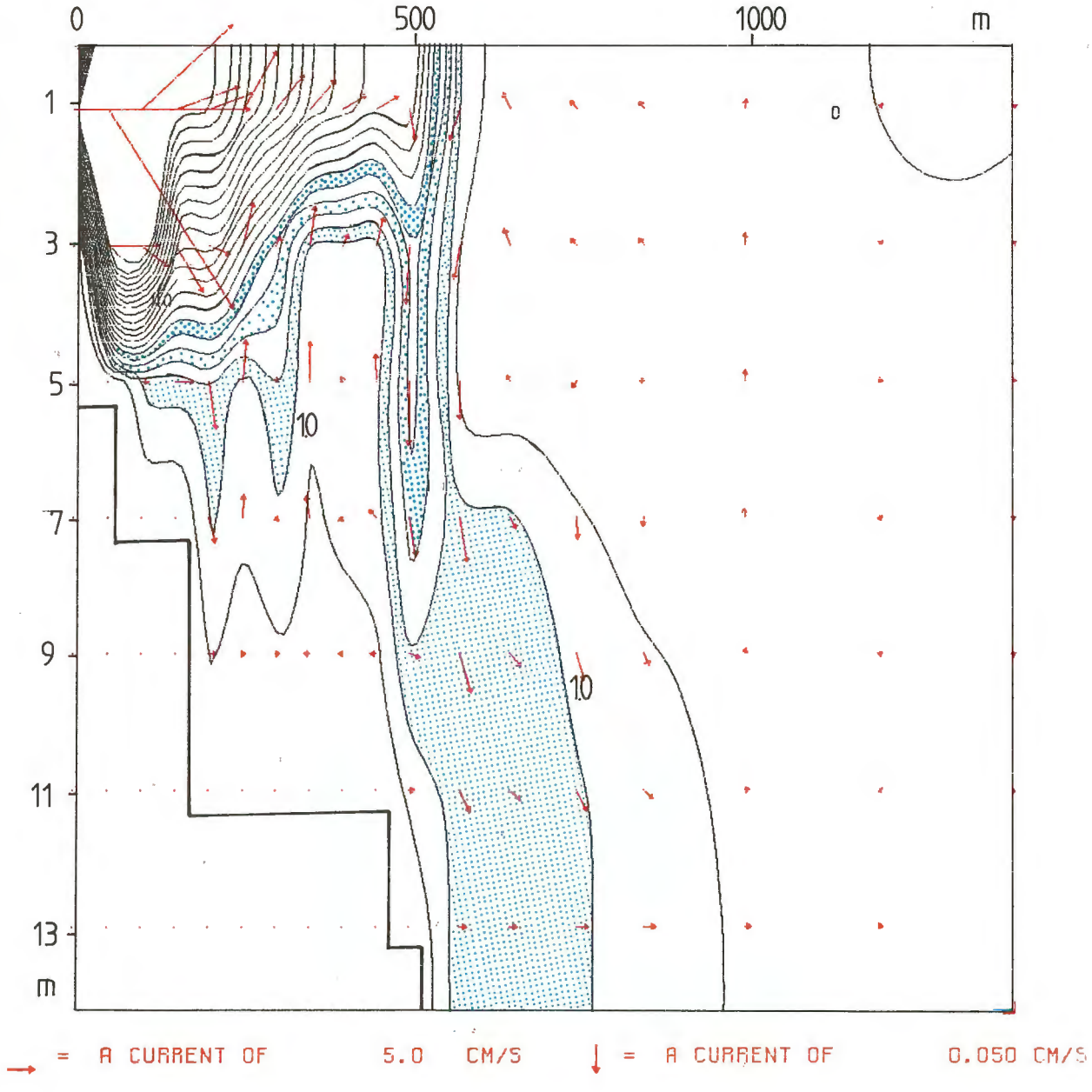

Fig. 20 A section out from the coast. (centerline)

For the grid cells close to the outlet this means

$$A_H = \frac{0.04 \cdot 50^2}{20} = 5 \text{ m}^2/\text{s}.$$

In a grid cell in an outer corner of the model the horizontal eddy viscosity coefficient A_H equals

$$A_H = \frac{0.04 \cdot 300^2}{\Delta t} = 180 \text{ m}^2/\text{s}.$$

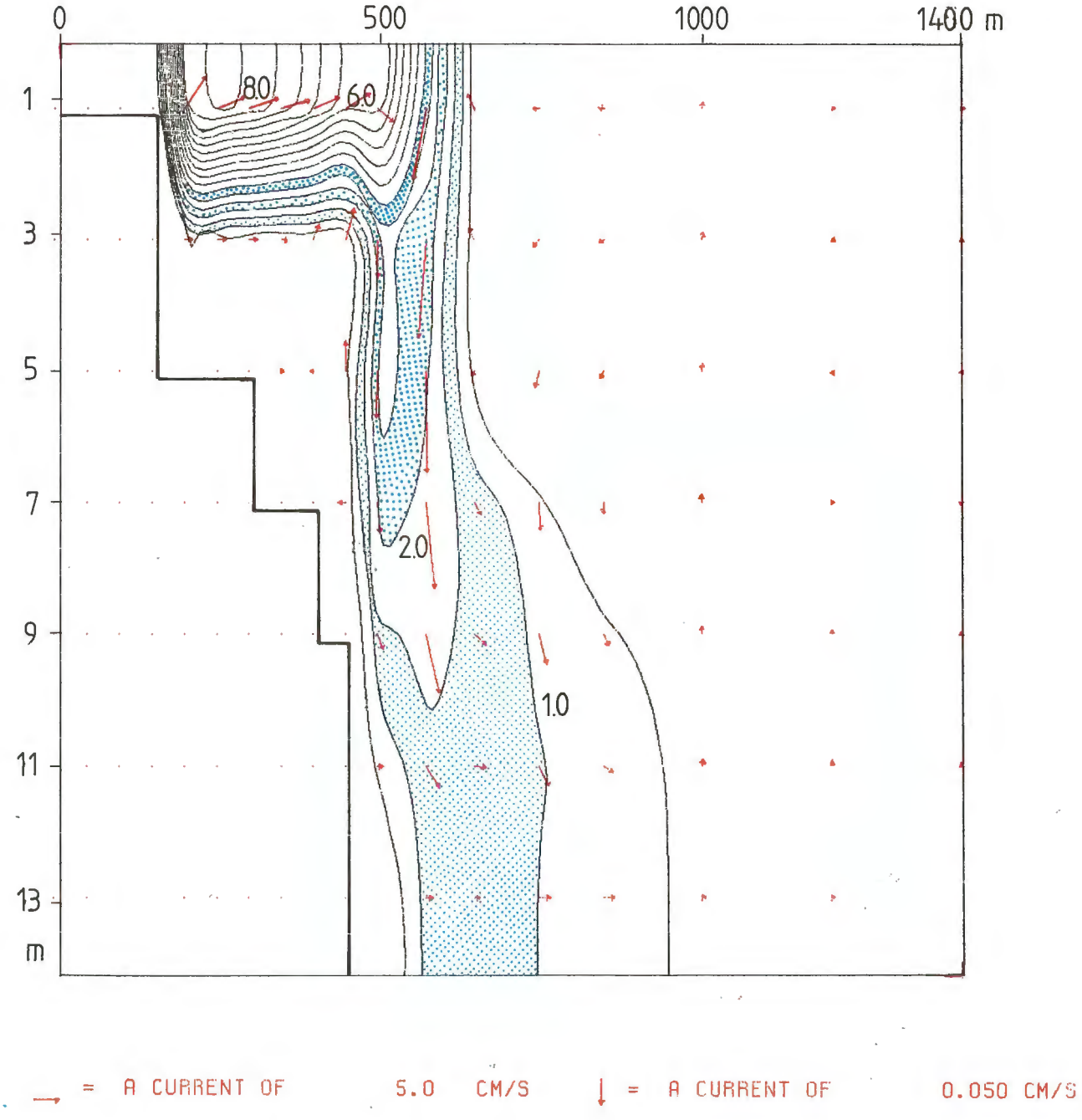

Fig. 21 A section out from the coast. (100 m north of the outlet)

It should be pointed out that in the model area of interest (around the cooling water plume) the grid size and the horizontal mixing is not significantly changed.

The centerline figure 20 shows the three different zones of the plume. 1) In the "jet" zone, where the plume is growing deeper, the vertical velocity at the centerline is downwards. So far the plume spreading is prohibited by the coast line.

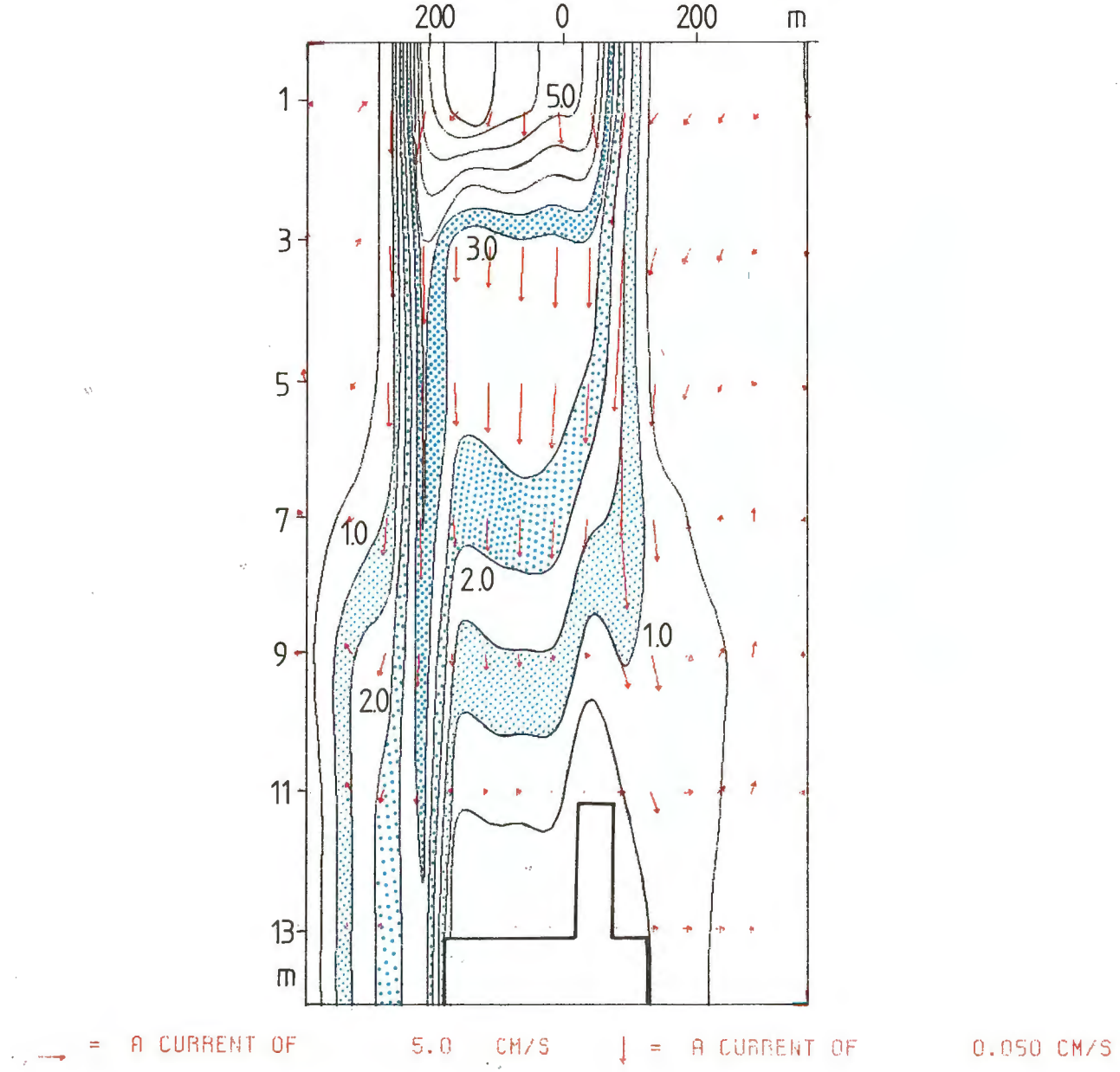

Fig. 22 A section along the coast 450 m from the shoreline.

2) In the "buoyancy" zone, where the main force is the buoyancy force, which makes the plume wide (as the coastline now allows for that) and thin, the vertical velocities are upwards. When the mixing goes on, the temperature in the plume comes close to the temperature for maximal density and 3) the zone of sinking water comes into play. The sinking takes place on both sides and in front of the plume, but it is most pronounced where the plume reaches deep water. The vertical velocities computed is below 0.5 cm/s. The maximum temperature at the bottom is computed to be 3°C. This is about the same bottom temperature that is computed in the cases with a more even bottom topography. Figures 20 to 24 display the plume and the velocity field.

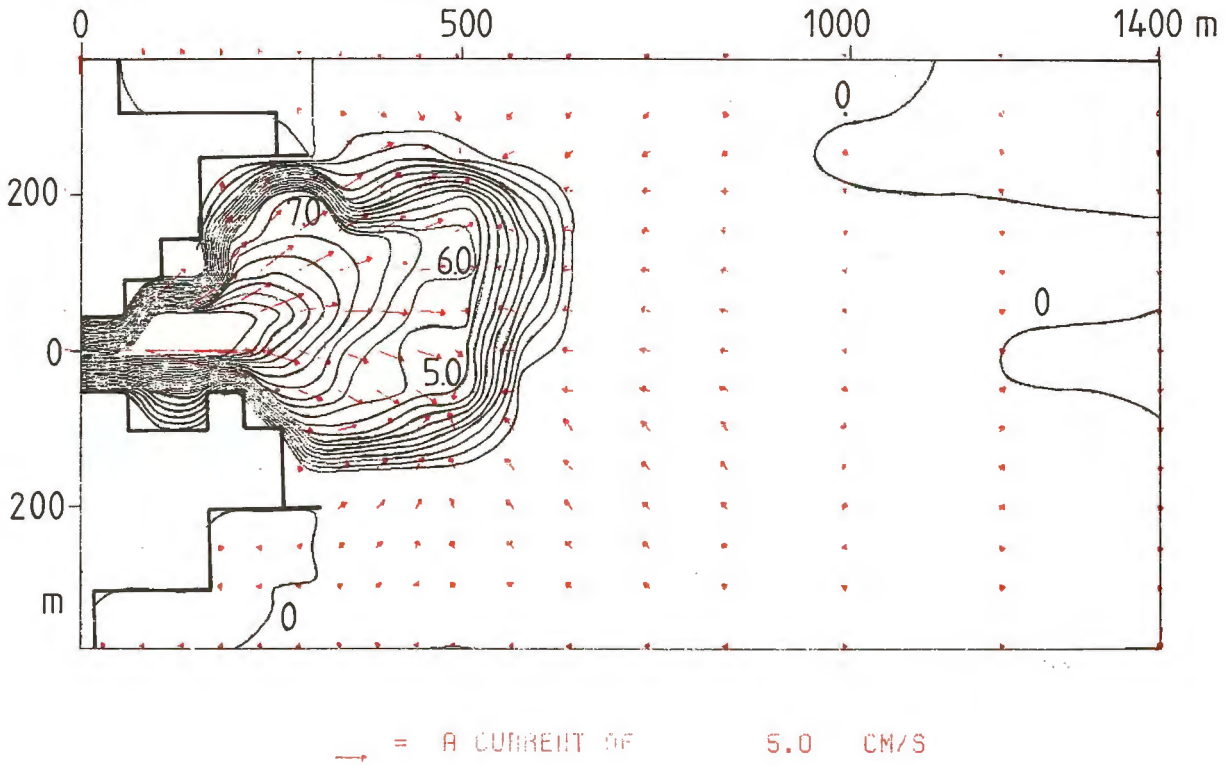

Fig. 23 The plume at the surface.

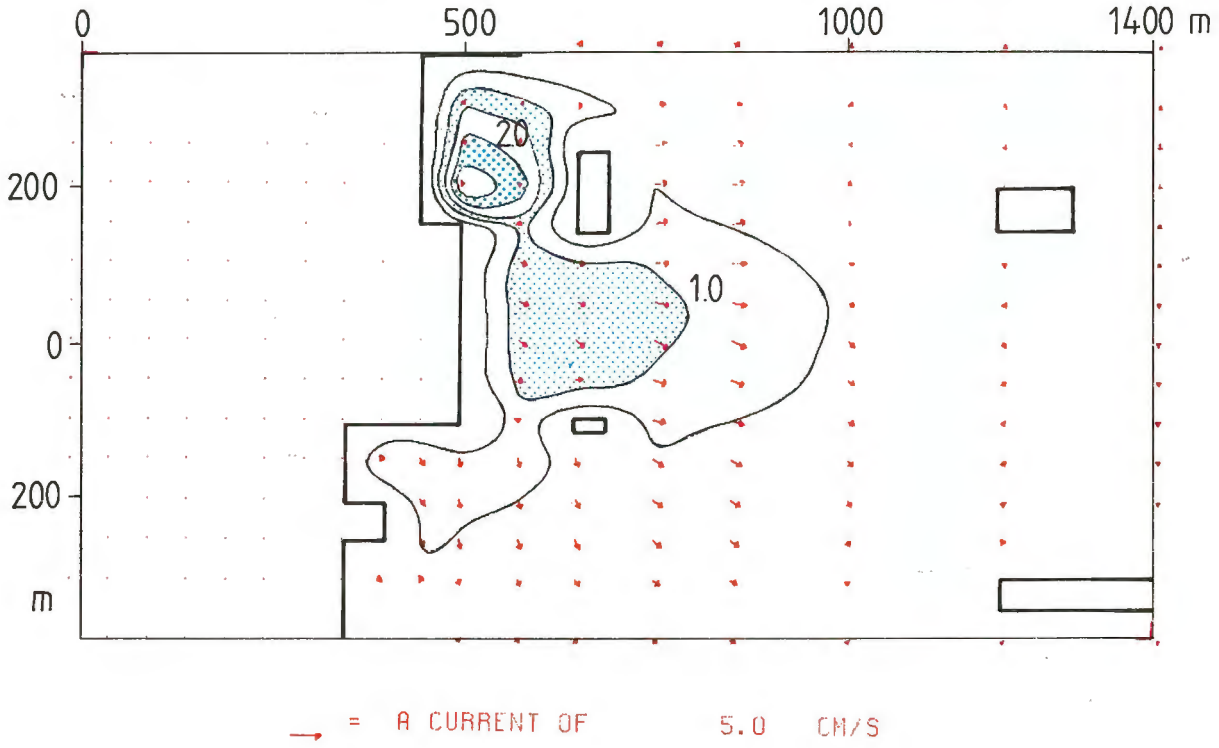

Fig. 24 The plume at the bottom 8 hours after the model start.

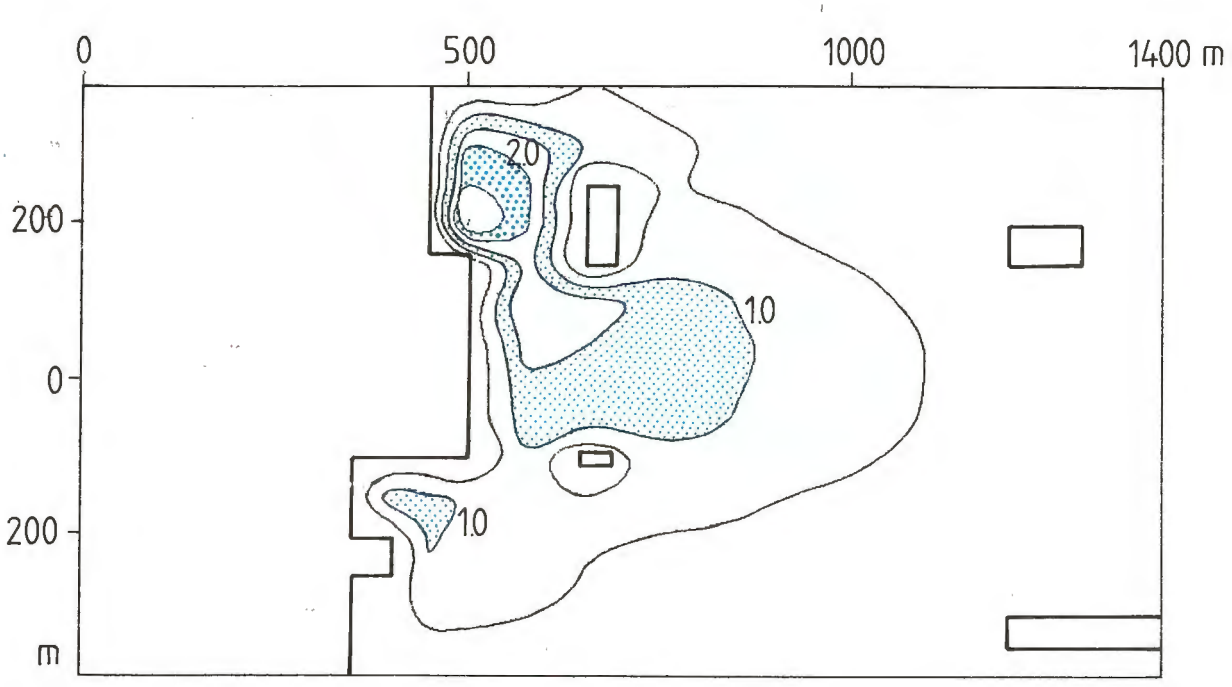

Fig. 25 The plume at the bottom 10 hours after the model start.

Figures 24 to 27 show a time evolution of the temperature field at the bottom. 8 hours after the model start the water begins to spread along the bottom. The flow at the bottom is blocked by the two shoals (see also figure 19).

After 10 hours the bottom temperature at the sinking spot is a little higher, and the spreading continues. Figures 26 and 27 show a quasi steady state with no change of temperature in the sinking region; the spreading along the bottom, however, continues.

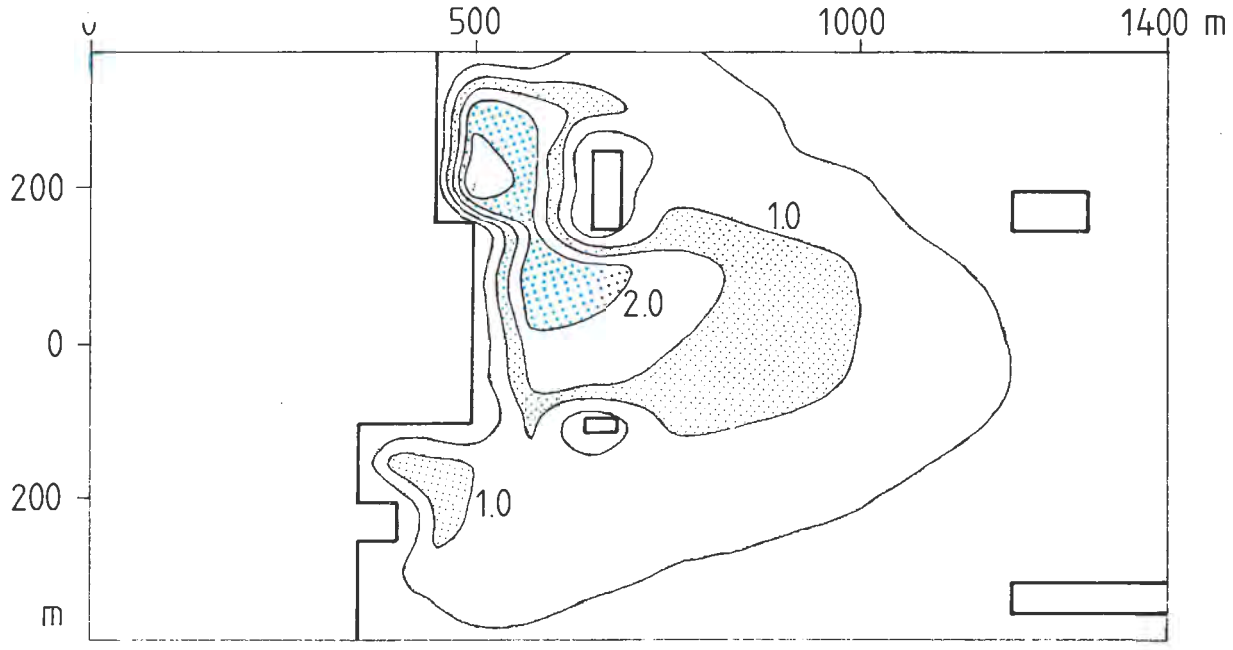

Fig. 26 The plume at the bottom 12 hours after the model start.

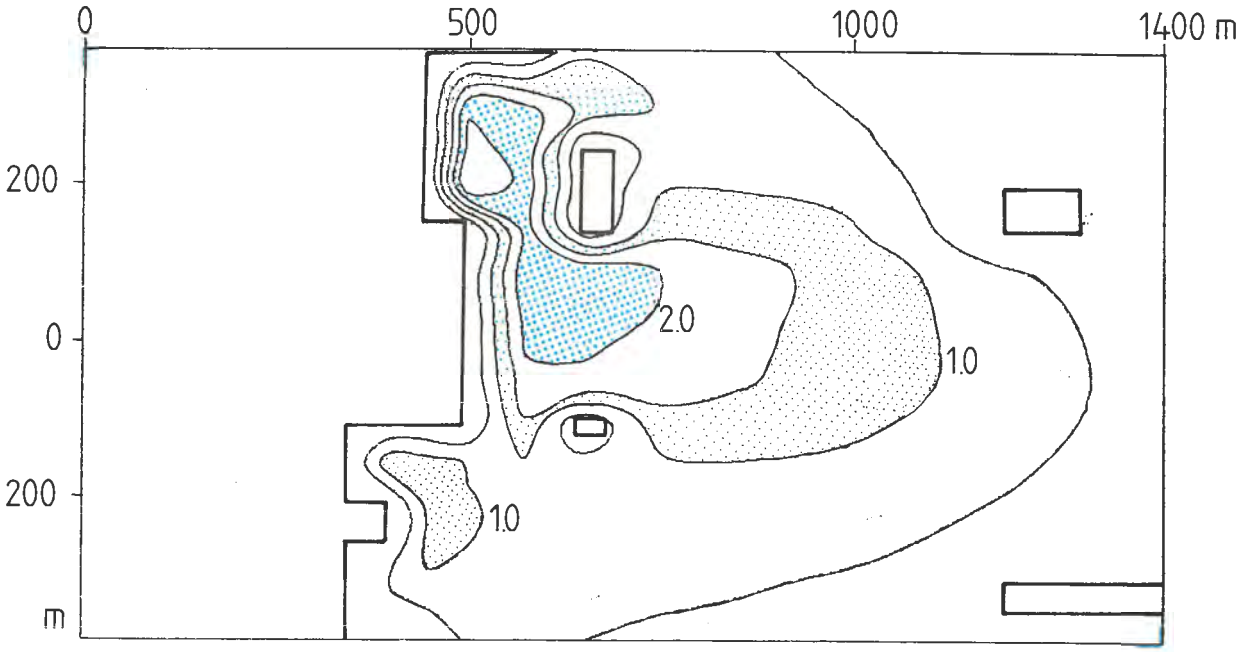

Fig. 27 The plume at the bottom 14 hours after the model start.

THE SPLITTING OF THE PLUME ALONG TWO AXES

The temperature pattern in figures 15 and 16 show an odd bifurcation. The plume has divided into two, and the highest temperatures are found along two diverging lines at the surface. This phenomena has a lot to do with the theory of smoke plumes in a cross flow (Turner, 1960). In Fischer et al. (1979) one can find pictures of buoyant laboratory plumes in a cross flow, where the bifurcation is clearly seen.

The splitted maxima is a result of a vortex around the line of maximum temperature or concentration. This vertical circulation pattern can be seen in figure 15. Two vertical eddies with rising water in common at the centerline can be traced. The theory for a jet in a cross flow can not be directly adapted for this case with quiescent water. Stefan et al. (1975) have pointed out experimental results, where secondary motion with upwelling along the centerline seems to exist in heated water plumes without cross flow. Stefan expects such flow to occur especially when the width of the plume is $\approx$ twice the depth. In other cases more than two vortices can develop. The grid spacing in this model does not allow more than two vortices in the plume, as the plume is not more than $\approx$ 200 m wide. The bifurcation in the computed results may therefore be extra pronounced.

CONCLUSIONS

Model studies of sinking plumes are carried out in a three-dimensional circulation model. Cooling water from a nuclear plant is ejected into the Baltic Sea of 0°C and 8 °/oo salinity. To get good predictions of temperatures and velocities in the plume, an exact knowledge of the vertical mixing is needed. It is shown that the velocity and temperature pattern of the plume is critically dependent on the vertical eddy viscosity coefficient used. A correct description of this vertical mixing does not jet exist.

However, approximate formulas to compute vertical mixing parameters from wind and from the density stratification and velocity shear are used. Thereby limits can be set for conditions, during which sinking can occur.

The cooling water can become denser than the ambient water if the ambient temperature is below 2 - 3°C (for fresh water 4°C). A pronounced sinking with a high-temperature core can persist, if the wind is around 1 - 2 m/s. If the wind velocity is higher, the plume is a diffuse one with slightly increased temperature from the surface down to the bottom. The plume does not reach far out from the outlet.

Bottom topography interacts with the sinking, so that higher sinking velocities and higher temperatures at the bottom have been computed for cases with complicated bottom topography than those for cases with flat bottom.

The few observed real sinking plumes have all been measured during calm wether conditions, which underpin the theoretical results. Observations of sinking plumes under ice are more numerous. This is explained by the fact that the turbulence under ice is believed to be weak.

The result of the computations shows that it is possible, in the three-dimensional model, to determine the extension of the geographical area that can be affected by sinking cooling water. It is also possible to forcast the time periods (% of the year, duration) when sinking will occur.

REFERENCES

Bork I, (1978): Preliminary model studies of sinking plumes SMHI Rapporter Hydrology och Oceanografi NR RHO 14(1978).

Brockmann C, Maier-Reimer, E, Meier-Fritsch, H (1978): An explicit numerical model to simulate events of upwelling. Symposium on the Canary Current: upwelling and Living Resources No 24/29, 1978.

Fischer M, et.al.(1979): Mixing in inland and coastal waters, Academic Press 1979.

Meier-Fritsch (1979): Ein Numerisches Modell des Nordwestafrikanischen Auftriebs. Distertation zur erlangung des Doktorsgrades der Mathematisch-Naturwissenschaftlichen Fakultät der Universität Hamburg.

Munk W, Andersson E, (1948): Notes on a theory of the thermocline. Journ. of Marine Res. VII, 3.

Neumann-Pierson (1966): Principles of Physical Oceanography. Prentice Hall 1966.

Nihoul J, (1975): Modelling of marine systems. Elsivier 1975.

Phillips N A, (1966): Boussinesq Approximation, Included in Thermal Convection: A Colloquium, National Center for Atmospheric Research, Boulder Colorado.

Stefan H, Bergstedt L, Mrosla E, (1975): Flow establishment and initial entrainment of heated water surface jets. US Environmental protection agency EPA-6601-75-014.

Turner J, (1960): A comparison between buoyant vortex rings and vortex pairs. J. Fluid Mech. No 7 (p 419-132)

Turner J, (1973) Buoyancy effects in Fluids. Cambridge Univ. Press.

Rapporter i SMHIs publikationsserier med anknytning till oceanografiska avdelningens verksamhet

Notiser och Preliminära Rapporter, serie Hydrologi

Nr 3 Karström, U

Infrarödteknik i hydrologisk tillämpning
Stockholm 1966

Nr 5 Ehlin, U & Nyberg, L

Hydrografiska undersökningar i Nordmalingsfjärden
Stockholm 1968

Nr 6 Milanov, T

Avkylningsproblem i recipienter vid utsläpp av kylvatten
Stockholm 1969

Nr 7 Ehlin, U & Zachrisson, G

Spridningen i Vänerns nordvästra del av suspenderat material från skredet i Norsälven i april 1969
Stockholm 1969

Nr 9 Ehlin, U & Carlsson, B

Hydrologiska observationer i Vänern 1959-1968 jämte sammanfattande synpunkter
Stockholm 1970

Nr 10 Ehlin, U & Carlsson, B

Hydrologiska observationer i Vänern 17-21 mars 1969
Stockholm 1970

Nr 11 Milanov, T

Termisk spridning av kylvattenutsläpp från Karlshamnsverket
Stockholm 1971

Nr 19 Holmström, H

Test of two automatic water quality monitors under field conditions
Stockholm 1972

Nr 20 Wennerberg, G

Yttemperaturkartering med strålningstermometer från flygplan över Vänern under 1971
Stockholm 1972

Nr 21 Prych, E

A Warm water effluent analyzed as a buoyant surface jet
Stockholm 1972

Nr 27 Wändahl, T & Bergstrand, E

Oceanografiska förhållanden i svenska kustvatten
Stockholm 1973

Nr 28 Ehlin, U

Kylvattenutsläpp i sjöar och hav
Stockholm 1973

Nr 36 Ehlin, U & Juhlin, B

Oceanografiska observationer runt svenska kusten med kustbevakningens fartyg 1979.
Norrköping 1980

Nr 38 Juhlin, B & Carlsson, B

Resultat och erfarenheter från försöksverksamhet med utökad vattenprovtagning från kustbevakningens båtar
Norrköping 1980

SMHI Rapporter

HYDROLOGI OCH OCEANOGRAFI

Nr RHO 1 — Weil, J G
Verification of heated water jet numerical model, Stockholm 1974

Nr RHO 2 — Svensson, J
Calculation of poison concentrations from a hypothetical accident off the Swedish coast, Stockholm 1974

Nr RHO 3 — Vasseur, B
Temperaturförhållanden i svenska kustvatten, Stockholm 1975

Nr RHO 4 — Svensson, J
Beräkning av effektiv vattentransport genom Sunningesund, Stockholm 1975

Nr RHO 5 — Bergström, S och Jönsson, S
The application of the HBV runoff model to the Filefjell research basin, Norrköping 1976

Nr RHO 6 — Wilmot, W
A numerical model of the effects of reactor cooling water on fjord circulation, Norrköping 1976

Nr RHO 7 — Bergström, S
Development and application of a conceptual runoff model, Norrköping 1976

Nr RHO 8 — Svensson, J
Seminars at SMHI 1976-03-29--04-01 on numerical models of the spreading of cooling water, Norrköping 1976

Nr RHO 9 — Simons, J, Funkquist, L och Svensson, J
Application of a numerical model to Lake Vänern, Norrköping 1977

Nr RHO 10 — Svensson, J
A statistical study for automatic calibration of a conceptual runoff model, Norrköping 1977

Nr RHO 11 — Bork, I
Model studies of dispersion of pollutants in Lake Vänern, Norrköping 1977

Nr RHO 12 — Fremling, S
Sjöisars beroende av väder och vind, snö och vatten, Norrköping 1977

Nr RHO 13 — Fremling, S
Sjöisars bärighet vid trafik, Norrköping 1977

Nr RHO 14 — Bork, I
Preliminary model studies of sinking plumes, Norrköping 1978

Nr RHO 15 — Svensson, J och Wilmot, W .
A numerical model of the circulation in Öresund. Evaluation of the effect of a tunnel between Helsingborg and Helsingör, Norrköping 1978

Nr RHO 16 Funkquist, L
En inledande studie i Vätterns dynamik, Norrköping 1978

Nr RHO 17 Vasseur, B
Modifying a jet model for cooling water outlets, Norrköping 1979

Nr RHO 18 Udin, I och Mattisson, I
Havsis- och snöinformation ur datorbearbetade satellitdata - en metodstudie, Norrköping 1979

Nr RHO 19 Ambjörn, C och Gidhagen, L
Vatten- och materieltransporter mellan Bottniska viken och Östersjön, Norrköping 1979

Nr RHO 20 Gottschalk, L och Jutman, T
Statistical analysis of snow survey data, Norrköping 1979

Nr RHO 21 Eriksson, B
Sveriges vattenbalans. Årsmedelvärde (1931-60) av nederbörd, avdunstning och avrinning

Nr RHO 22 Gottschalk, L and Krasovskaia, I
Synthesis, processing and display of comprehensive hydrologic information

Nr RHO 23 Svensson, J
Sinking cooling water plumes in a numerical model Norrköping 1980